ABSTRACT

Thesis: ESTIMATION OF LONG TERM BRIDGE PIER SCOUR
                                 IN COHESIVE SOILS AT MARYLAND BRIDGES
                                 USING EFA/SRICOS

                                 Veronica M. Ghelardi, Master of Science
                                 Civil Engineering, 2004

Thesis Directed by: Professor Kaye Brubaker
                                 Department of Civil Engineering

                                 Professor Deborah Goodings
                                 Department of Civil Engineering

Estimation of scour in cohesive soils is based on equations developed for non-cohesive

soils that produce conservative scour estimates when applied to cohesive soils. This

thesis evaluates the development of bridge pier scour via SRICOS, Scour in Cohesive

Soils, a method to determine bridge pier scour depth in cohesive soils using results of the

Erosion Function Apparatus (EFA) erosion tests and a hydrograph. Soil samples were

collected from five Maryland sites; the EFA was used to measure their erosion rates and

the SRICOS software predicted scour depths over a user-determined timespan. Predicted

scour depths were compared to HEC-18 predicted pier scour depths. In all instances, the

EFA/SRICOS method predicted less scour than the HEC-18 method, the current design

standard. EFA/SRICOS represents an emerging re-thinking of erosion characterization to

predict scour depths of cohesive soils at piers.

ESTIMATION OF LONG TERM BRIDGE PIER SCOUR IN COHESIVE SOILS AT
MARYLAND BRIDGES USING EFA/SRICOS

by

Veronica M. Ghelardi

Thesis submitted to the Faculty of the Graduate School of the
University of Maryland, College Park in partial fulfillment
of the requirements for the degree of
Master of Science
2004

Advisory Committee:

Professor Kaye Brubaker
Professor Deborah Goodings
Professor Gregory Baecher

Table of Contents

List of Tables

'List of Figures

1. INTRODUCTION

1.1 Background

Scour is the removal of soil caused by water flowing over a soil surface. When scour occurs at a bridge structure, the scour may undermine the foundations, ultimately resulting in structural failure. This was the cause of a 1987 New York bridge failure over Schoharie Creek, which resulted in the loss of 10 lives, and the 1989 Tennessee Hatchie River bridge failure in 1989, which resulted in eight lives lost. Although these are extreme cases, these failures illustrate scour's potentially devastating effects.

The failure of these two bridges in 1987 and 1989 prompted the Federal Highway Administration to mandate scour prevention on all federally funded bridge projects. Typically, in order to prevent undermining of foundations, most bridge foundations are designed to extend well below the estimated scour depth. There has been much scour research in coarse or sandy soils, but relatively little comparable scour research in cohesive soils such as silts and clays. Sandy soils are known to erode particle by particle, while cohesive soils usually erode in clumps rather than individual particles. However, the bonding mechanism of cohesive soils is little understood from one cohesive soil to another. Studies, reviewed in section 2.2, reveal that soil type, water temperature, salinity, plasticity index, liquid limit, and molecular bonding are among some of the parameters that may have some effect on the bonding of cohesive soils. Other studies, also reviewed in section 2.2, report results that appear to contradict some of these findings. Because this bonding is so complex, no set of equations to predict scour depths in cohesive soils has been widely accepted.

The Federal Highway Administration has recommended use of the HEC-18 equations to estimate maximum scour depths at structures. These equations were developed to estimate scour in non-cohesive soils. The prevailing assumption is that cohesive soils will scour to the same depth as non-cohesive soils, although it will take longer to reach the same scour depths, sometimes longer than the life of the bridge. Non-cohesive equations may provide a margin of safety for foundation depths in cohesive soils that result in unnecessary expense if the scour depths do not reach the maximum non-cohesive predicted scour depths within the life of the bridge.

A new method called Scour Rate in Cohesive Soils (SRICOS, Briaud et al. 1999) attempts to estimate maximum cohesive soil scour at bridge piers empirically. The SRICOS method relies on measuring the erosion rate for site-specific soils in the laboratory using a modified flume called an Erosion Function Apparatus (EFA).

The EFA endeavors to determine the amount of erosion as a function of flow velocity. In concept, the EFA allows the user to determine the critical shear stress of the in-situ soil. This information is combined with a stream velocity hydrograph for some design period, for example for the expected life of the bridge plus 20%, to predict the pier scour depth over the desired time period. Since this method uses a direct measure of erosion and does not rely on soil composition parameters for prediction, it does not delve into the reasons for the soil cohesiveness or the conditions that will produce scour in the soil other than the critical shear stress required for particle movement. Water temperature and salinity and soil properties such as the clay-silt ratio are not included as input parameters to this method.
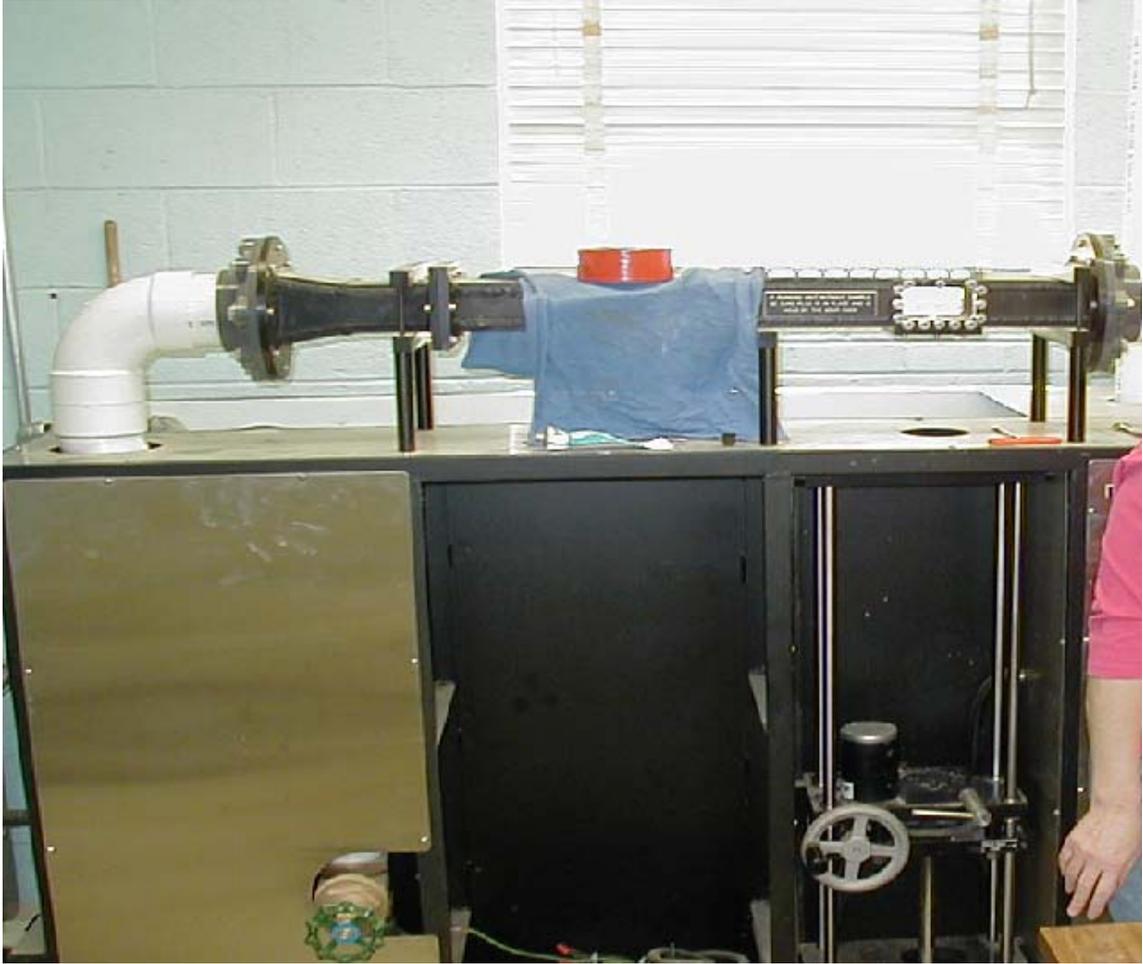
Figure 1.1. Erosion Function Apparatus

SRICOS is the only known method currently available that estimates scour depth as a function of time. Under the prevailing assumption that cohesive soils require more time to reach their maximum scour depths than non-cohesive soils, if a time factor could be incorporated into the scour equations then it might be possible to design foundations that need only be as deep as the scour depth that can be expected over the life of the structure. A driving force for bridge owners to adopt better scour estimate methods would be to reduce the foundation depth and thereby save money when building new, but still safe structures.

1.2 Research Goals

The research reported in this thesis contributed to a study with the goal of evaluating Briaud et al.'s (1999) method to predict bridge pier scour in cohesive soils in terms of its applicability to bridge crossing sites in Maryland. The method, known as EFA-SRICOS, was developed at the University of Texas, using soils and streams in Texas. The current study is part of a larger project to evaluate the method in different regions of the country. The study consisted of three stages: (1) using the Erosion Function apparatus (EFA) to characterize cohesive soils at selected bridge crossing sites in Maryland; (2) developing a method to generate synthetic discharge hydrographs for ungaged sites in Maryland to provide the required inputs to SRICOS; and (3) based on inputs from the first two stages, using the SRICOS method to predict bridge pier scour at the selected sites. This thesis comprises stages 1 and 3. Stage 2 was performed at the University of Maryland by other personnel, and is briefly described in this thesis as relevant to stages 1 and 3.

The study follows the procedures outlined in reports by Briaud, et al. (2003) for the Texas Department of Transportation Construction Division. The EFA-SRICOS results are compared to the currently used HEC-18 equations for pier scour estimation.

2. LITERATURE REVIEW

2.1. Physical Fundamentals

Flowing water over sediment exerts forces on streambed sediments that tend to move or entrain the sediments. These forces have two components: the tangential force, drag, and the normal force, lift. Drag results from viscous stresses at low velocities but at high velocities the pressure differential between the upstream and downstream face of the particle is the principle force moving the particles (Leopold, 1994). Finer sediments composed of cohesive soils such as silt and clay resist movement mainly by cohesion.

Critical condition is defined as the point when the fluid force acting on a grain of sediment or on particles of cohesive sediment reaches a value that puts the particle into motion. Particle movement first appears erratic and is the result of the unstable grain position relevant to other particles. At some point movement becomes more general, determining the point at which the critical condition is reached. Data available on critical shear stress are based on what seem to be subjective definitions of critical conditions. However, observers asked to decide when general movement has occurred, will pick a point that is within a few percent of the same velocity, (Henderson 1966).

Early Shear Stress Studies. Flume experiments on critical shear stress for non-cohesive sediments show that the motion of sediment grains on the bed is highly unsteady and non-uniformly distributed over the bed area.

The drag force is predominant in turbulent flows when the Reynolds number (D_sV/v) is high. In laminar flow the shear force is predominant and the Reynolds number is small. The ratio of the forces that move a particle to that of the forces that resist movement is:

$$\tau_o/(\gamma_s-\gamma)D_s \hspace{8cm} (2.1)$$

where: τ_o = average shear stress

γ = specific weight of water

γ_s = specific weight of the sediment

D_s = diameter of sediment particle

Shields (1935) experiments of incipient motion determined the relationship between the Reynolds number, $V\,D_s/\upsilon$ and $\tau_o/(\gamma_s-\gamma)D_s$, known as the Shields relation. His experiments led to the development of the widely-accepted Shields diagram to determine the incipient motion shear stress. Fig. 2.1 (FHWA,HD-6 2001)
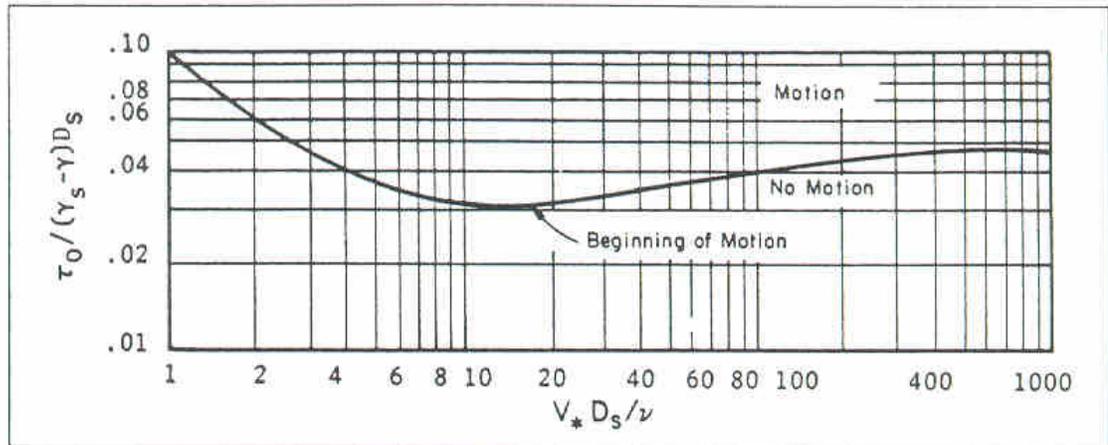
Figure 2.1 Shields Diagram (FHWA,HD-6 2001, after Gessler 1971)

Critical Velocity. Particle movement in steady, uniform flow begins when the shear stress equals the resistance forces on the particle.

The velocity profile for a two-dimensional free-surface flow over a flat sediment bed is given by:

$$U/U_* = a_r + 5.75 \log y/k_s \tag{2.2}$$

where

U = the velocity at distance y above the bed

y = any distance above the bed

U* = critical velocity, flow at which particle movement begins

k_s = the characteristic roughness of the sediment size

a_r = a function of the boundary Reynolds number

Equation 2.2 shows that if two flows of different depth have flat beds of identical sediment and the same bed shear stress, the velocities at any distance y above the bed will also be the same in the two flows. However, because the mean velocity occurs at y equal to a constant fraction of the depth, the deeper flow will have the larger mean velocity. To determine the scouring action of the water at the bed, the mean velocity and depth of the bed must also be given. The bed condition can also be specified by a velocity at a given value of y. The advantage of using shear stress to identify critical conditions is that only one variable is necessary.

Relations between velocity, depth, and particle resistance have been developed from equating shear stress to resistance. The average bed shear stress can be found by the equation:

$$\tau_o = \gamma \, R \, S \tag{2.3}$$

where: γ = unit weight of water

R = hydraulic radius

S = slope

If y is substituted for R and the Mannings equation:

$$V = 1.49 R^{2/3} S^{1/2} / n \qquad\qquad (2.4)$$

is used to find the slope, then equation 2.3 becomes :

$$\tau_o = \rho g\, y S_f = \rho g\, n^2 V^2 / (1.49)^2\, y^{1/3} \qquad\qquad (2.5)$$

The Shields relation can be used to determine the relation between the critical shear stress and the bed material size for incipient motion. That relation is:

$$\tau_c = K_s\, (\rho_s - \rho)\, gD \qquad\qquad (2.6)$$

If the applied shear stress equals the critical shear stress:

$$\tau_o = \tau_c \qquad\qquad (2.7)$$

then

$$\rho g\, n^2 V^2 / 2.22\, y^{1/3} = K_s(\rho_s - \rho) g\, D_s \qquad\qquad (2.8)$$

> where: y = average depth of flow
>
> S_f = slope of the energy grade line
>
> V = average velocity
>
> D_s = diameter of particle
>
> n = Mannings coefficient
>
> K_s = Shield's coefficient of .039, an average value for all size materials
>
> (Fiuzat& Richardson 1983, Ruff etal., 1985, 1987)

To find the critical velocity equation 2.8 can be rearranged:

$$V_c = (1.49\, K_s^{1/2}\, (S_s - 1)^{1/2}\, D_s^{1/2}\, y^{1/6}\,)/ n \qquad\qquad (2.9)$$

$$n = K_{nu}\, D_s^{1/6} \qquad\qquad (2.10)$$

$$K_{nu} = 0.0336 \quad \text{(FHWA, HD-6,2001)} \qquad\qquad (2.11)$$

Then $\ V_c = K_u\, D_s^{1/3}\, y^{1/6} \qquad\qquad (2.12)$

$$K_u = 1.49\ K_s^{1/2}\ (S_s - 1)^{1/2}/\ K_{nu} \qquad\qquad (2.13)$$

These equations are for steady, uniform flow and FHWA's HD-6 (2001) recommends their use to find the critical depth and size for incipient motion based on the Mannings equation, specific gravity of the particles and the Shield's parameters.

Lift on Particles. As reported by ASCE (1977), Einstein and El-Samni (1949) and Apperley (1968) made the only quantitative observations of lift on sediment in a bed. Einstein and El-Samni (1949) measured the difference in mean static pressure in sediment beds at the bottom of the top layer of sediment and at the wall of the channel at the top of the top layer of sediment. In these experiments the velocity was less than the critical velocity and no sediment moved. Their measurements yielded a pressure difference or lift pressure, Δp, on the grains given by

$$\Delta p = 0.178\ *(.5\rho\ u_o^2) \qquad\qquad (2.14)$$

where

u_o = the velocity equal to the distance of the height of the d_{35} particle

above the bed

d_{35} = size of grains for which 35% by weight of the bed material is finer

The Reynolds values in the experiments used to obtain Eq. (2.14) were approximately 50,000. Therefore, the lift pressure given by Eq. (2.14) should be valid only for rough boundaries.

2.2. Scour in Cohesive Soils

A literature search reveals that there is relatively little research of scour in cohesive soils. The factors that result in cohesive soils seem to be many and varied as

reported by a number or researchers over the years. It is clear from the research that sediment properties that determine its resistance to erosion are not completely defined.

According to ASCE (1968), Dunn (1959) determined the critical shear stress for sediments ranging from sand to silty clay taken from several channels in the Western U.S. He applied a submerged jet of water directed vertically downward onto sample sediments. He concluded that increasing clay content increases the critical shear stress. Further, ASCE reports that Smeardon and Beasley (1961) determined the critical shear stress for 11 cohesive soils. They concluded that the plasticity index and the percentage of clay in the soils had an effect on the shear stress. However, these conclusions were disputed by Flaxman (1963), who reported that, although some researchers had found a relation between high plasticity index and high resistance to erosion, he examined several natural channels and found that low- or no-plasticity soils exhibited high resistance to erosion. Flaxman examined soil permeability and unconfined compression tests as indicators of erodilibility of clay, however, it is difficult to make an argument supporting why these would be reliable indicators.

Grissinger and Asmussen (1963) found that the erosion resistance of clay soils varied with the type and amount of clay minerals, orientation, bulk density and antecedent water content and the water temperature.

The ASCE (1977) report described research by Abdel-Rahmann (1964) who studied the erosion resistance of clayey sediments. The clay used in these experiments was high in silicate content (more than 90%) and of a type that swells when it absorbs water. The conclusion was that the erosion process was independent of shear stress and was related to the swelling of the clay.

Grissinger (1966) studied the properties of certain clays that are resistant to erosion. He concluded that the type and amount of clay present in the soil, as well as the orientation of the clay particles and the temperature of the eroding water, all vary the ability of the cohesive soil to resist erosion.

Kuti (1976) found that the ultimate volume of soil scoured, regardless of the percentage of clay mineral present, was the same. However, the in-situ void ratio determined the length of time it took to reach the equilibrium scour depth. He also found that the percent clay in a soil and its plasticity index can be used as indicators of soil resistance to erosion.

Kamphuis (1989) studied the influence on erosion in a cohesive bed of the non-cohesive material carried by the streamflow. The sediment transport characteristics of an eroding fluid containing a granular material greatly influences the erosion of the cohesive material. He found this to be true in all cases except in absolutely clear water. Kamphuis further states that if granular materials are present in the stream or granular material overlays a cohesive soil in a discontinuous layer, the design should be based on the sediment transport characteristics of the granular material.

Briuad etal (1999) discussed a study of cylindrical pier scour in cohesive soils that predicted scour depth versus time for a constant velocity flow. Shelby tube soil samples are tested in an Erosion Function Apparatus, EFA, to obtain an erosion rate versus shear stress curve. This method of scour prediction in cohesive soils is discussed in depth later in this chapter.

Guven et al. (2003) discussed a simplified theory of bridge scour in cohesive soils over time in clear water based on Briaud's (1999) "scour rate in cohesive soils" concepts.

11

Guven et al. developed a differential equation based on Briaud's empirical rate of erosion for the dependence of the flow depth at time t.

Molinas et al. (1996) studied the magnitude and geometry of the equilibrium local scour at a bridge pier in cohesive soil. Their results showed in part that the scour depth decreased as the clay/sand ratio increased up to 40%. Beyond this clay content, other factors such as compaction, water content, etc. become more critical to the ability of the soil to resist erosion. They also found that the higher the clay content, the longer it takes to reach the equilibrium scour depth and the steeper the slope of the scour hole. They also argued that as the initial soil water content decreases the scour depth decreases. This study is not directly applicable to in situ clays because Molinas made his own clay and let it set up for only a few days as opposed to in situ clays that have been compressed by natural forces.

Annandale's (1999) Erodibility Index Method estimates pier scour in rock and other scour-resistant soils. The method is based on stream power (average velocity times bed shear stress) and soil resistance to erosion. The erosion resistance is defined by the Erodibility Index, a geo-mechanical quantifier. Scour stops when the erosive power required to scour exceeds the available erosive power.

Ansari et al. (2002) state that there is little known about the effect of cohesive material on pier scour. As other researchers have found, the point at which a cohesive material is eroded is difficult to predict because it varies with the type and percentage of the clay content, compaction and/or consolidation. Their monitoring of scour holes revealed that sediments with clay content between 5% and 10% scoured first from the sides of the pier, then the scour holes propagated upstream along the sides of the pier and

12

met at the nose of the pier. The scour depth increased rapidly and created the deepest

scour hole at the pier nose.

In their studies of erodibility of cohesive streambeds in the Midwestern U.S.,

Hanson and Simon (2002) found that correlations to individual soil characteristics such as

plasticity index, undrained shear strength and gradation were poor and can only be rough

indicators of erodibility. They agreed with the Briaud (2001) conclusions that there is no

generally accepted correlation between measured soil parameters and erodibility and thus

a direct measurement method is better.

2.3. Current methods to estimate bridge pier scour

Current methods for determining scour at bridge piers in cohesive soils rely on

equations for scour in sandy soils, based on the assumption that cohesive soils will scour

to the same depth as non-cohesive soils but will take much longer to reach the maximum

scour depth. This section summarizes these methods.

Melville and Chiew (1999) conducted experiments on uniform sands to develop

an equation for equilibrium scour depth at a bridge pier as a function of time in clear

water scour. They concluded that equilibrium scour depth is approached asymptotically,

that scour depths after 10% of the time to equilibrium has passed achieved 50% to 80%

of the equilibrium scour depth, and that time to equilibrium is a function of flow

intensity, flow shallowness and sediment size. Their equations can be used to estimate

the scour depth at any stage of the scour hole development.

HEC-18 (FHWA 2002) is a method of calculating scour in sandy soils.

According to the HEC-18 manual, the foundation of scour equations is conservation of

mass in sediment transport: there must be an equilibrium of sediment and water flow into

and out of a cross section. As the scour hole enlarges and increases the flow area, the shear stress and average flow velocity decrease. This describes the point of maximum scour depth in the case of live bed scour. In the case of clear water scour no sediment is transported into the cross section and the maximum scour depth is reached when the critical shear stress of the bed material is reached.

HEC-18 uses a modified Colorado State University (CSU) equation recommended by FHWA's Interim Procedures Technical Advisory T5140.20. The modification includes coefficients for the effects of bed form and bed size material. When the equation was compared to USGS field data, it was found to produce conservative scour depths that provided a built-in margin of safety.   The resulting HEC-18 equation is used for both clear water and live-bed scour pier scour and predicts the maximum pier scour depths. The equation is:

$$y_s/y_1 = 2.0 \ K_1 \ K_2 \ K_3 \ K_4 \ (a/y_1)^{0.65} \ Fr_1^{0.43} \qquad (2.15)$$

where:

y_s = scour depth

y_1 = flow depth directly upstream of the pier

K_1 = correction factor for pier nose shape

K_2 = correction factor for angle of attack of flow

K_3 = correction factor for bed condition

K_4 = correction factor for armoring by bed material size

a = pier width

L = length of pier

Fr_1 = Froude Number directly upstream of the pier $= V_1 / (gy_1)^{0.5}$

V_1 = mean velocity of flow directly upstream of the pier

g   = acceleration of gravity (9.81 m/s^2) (32.2 ft/s^2)

Eq. (2.15) applies to scour in non-cohesive soil (sand). The correction factors (K1 through K4) are based on bridge geometry and steam bed characteristics and can be determined from look up tables in the HEC-18 manual.

2.4. The EFA/SRICOS Method

A study of pier scour in cohesive soils sponsored by the Texas Department of Transportation (Briaud et al. 2003) proposed a method to predict scour as a function of time. The method combines information on soil properties obtained from a modified flume called the Erosion Function Apparatus, EFA, the flow velocity in front of the pier obtained from a hydraulics software program such as HEC-RAS, a discharge hydrograph obtained from USGS gage sites, and their SRICOS software (Briaud et al. 2003). The underlying concept of this study is that, since cohesive soil bonding is so complex and not easily understood, a better approach is to remove site-specific soils in as undisturbed condition as possible and through direct erosion tests determine the critical shear stress of the soil. This information, combined with a velocity hydrograph of the site, should give a more realistic estimate of the maximum scour depth. The EFA-SRICOS methods are the focus of this thesis and are discussed in detail in Chapter 3.

3. METHODS

Five test sites with cohesive soils at the bridge piers were selected to test the SRICOS method for pier scour under Maryland conditions. Samples from the sites were analyzed using the Erosion Function Apparatus (EFA) to obtain the required entry data for the SRICOS program. Four of the five sites are ungaged; therefore, a synthetic hydrograph procedure was used to produce the required time series of discharge for input to the SRICOS program. The scour depths predicted by SRICOS were compared to scour depths obtained from the commonly used Federal Highway Administration HEC-18 method. This chapter describes the procedures used for each of these steps.

3.1. Site selection

Maryland State Highway Administration geotechnical engineers identified areas in Maryland most likely to have cohesive soils. According to these sources, cohesive soils are primarily in the Piedmont and Coastal Plain Regions of Maryland extending through Montgomery, Frederick, Howard, Anne Arundel, and Carroll counties.

Figure 3.1 MD 28 over Seneca Creek (existing bridge)

Figure 3.2 MD 355 over Great Seneca Creek (existing bridge)

Figure 3.3 MD 26 over Monocacy River (existing bridge)

Figure 3.4. MD 7 over White Marsh Run (existing bridge)

Figure 3.5. I-95 over Potomac River (rendered drawing of proposed bridge)

All MSHA owned bridges in the selected region were identified and the soil boring logs scrutinized for clay material at the piers. The selected study sites were MD 28 over Seneca Creek (Figure 3.1), MD 355 over Great Seneca Creek (Figure 3.2), MD 26 over Monocacy River (Figure 3.3), MD 7 over White Marsh Run (Figure 3.4) and I-95 over the Potomac River, aka Woodrow Wilson Bridge (Figure 3.5). The study sites are sumarized in Table 3.1.

Table 3.1. Study Sites

Site	Water Crossing	County	Number of Samples
MD 28	Seneca Creek	Montgomery	4
MD 355	Great Seneca Creek	Montgomery	2
MD 26	Monocacy River	Frederick	2
MD 7	Whitemarsh Run	Baltimore	4
MD I-95	Potomac River (Woodrow Wilson Bridge)	Border of Prince Georges County & Virginia	2

It is MSHA policy to minimize channel degradation at bridge crossings by placing bridge piers in the overbanks where possible. Consequently, three of the bridge sites selected (MD 28 over Seneca Creek, MD 355 over Great Seneca Creek and MD 7 over White Marsh Run) have piers in the overbanks. This policy required modifications to be made in the SRICOS method that are detailed later in this chapter.

3.2. Analysis of Soil Properties

Samples were obtained using an ASTM standard Shelby tube with a 76.2 mm outside diameter. If a sample could not be taken near the pier, then the sample was taken from the overbank in the same soil layer as the pier. MSHA personnel collected Shelby tube samples from each site and the sample soil trimmings were tested by the MSHA soils lab for identification of soil type, D_{85}, D_{50}, D_{35}, Atterberg Limits (Plasticity Index, Plastic Limit, Liquid Limit), and the content of gravel, sand, silt and clay. The Atterberg Limits are used to describe the ability of a fine-grained soil to absorb water. The plastic limit defines the water content at point of transition of the soil from semisolid to plastic state. The liquid limit defines the water content at the point of transition of the soil from plastic to liquid state.

3.3. EFA Test of Soil Samples

As described in the SRICOS Research Report 2937-1 (Briaud, 1999) the sample tube was placed on the EFA piston, the soil sample trimmed flush to the top of the tube, and then fed through a circular hole until flush with the bottom of the flume and sealed with an O-ring. The flume is a 4" x 2" rectangular pipe with flow straighteners at the upstream end to reduce turbulence.

Once the tube was securely set in place and the water pump was turned on, the velocity was set to the desired speed and the sample was pushed into the flow 1 mm. As the sample eroded, the 1mm protrusion of the sample soil in the flow was maintained by manually advancing the piston. The sample was tested for 1 hour or 50mm of erosion, whichever came first. At the end of the test the sample was removed from the flume, re-trimmed flush to the tube and the procedure was repeated for up to 8 tests at velocities of 0.3m/s, 0.6m/s, 1m/s, 1.5m/s, 2m/s, 3m/s, 4.5m/s, and 6m/s. Erosion results from the 6m/s velocity were regarded as unreliable due to the opaqueness of the water and the inability to see the sample and push it in a timely manner. The erosion and calculated shear stress were recorded for each velocity. The data obtained was used to plot the erosion rate vs. velocity curve and the shear stress vs. velocity curve for each soil sample; this information is required for the SRICOS program. The erosion recorded for each test was used to calculate the erosion rate in mm/hr. The shear stress at the selected critical shear stress was determined according to the SRICOS method by calculating the shear stress from the Moody Chart for pipe flows.

$$\tau = f\rho v^2/8 \qquad\qquad\qquad (3\text{-}1)$$

where: v = mean flow velocity

ρ = mass density of water

f = friction coefficient whose value corresponds to the Reynolds number, Re, and

the soil surface roughness ε /D.
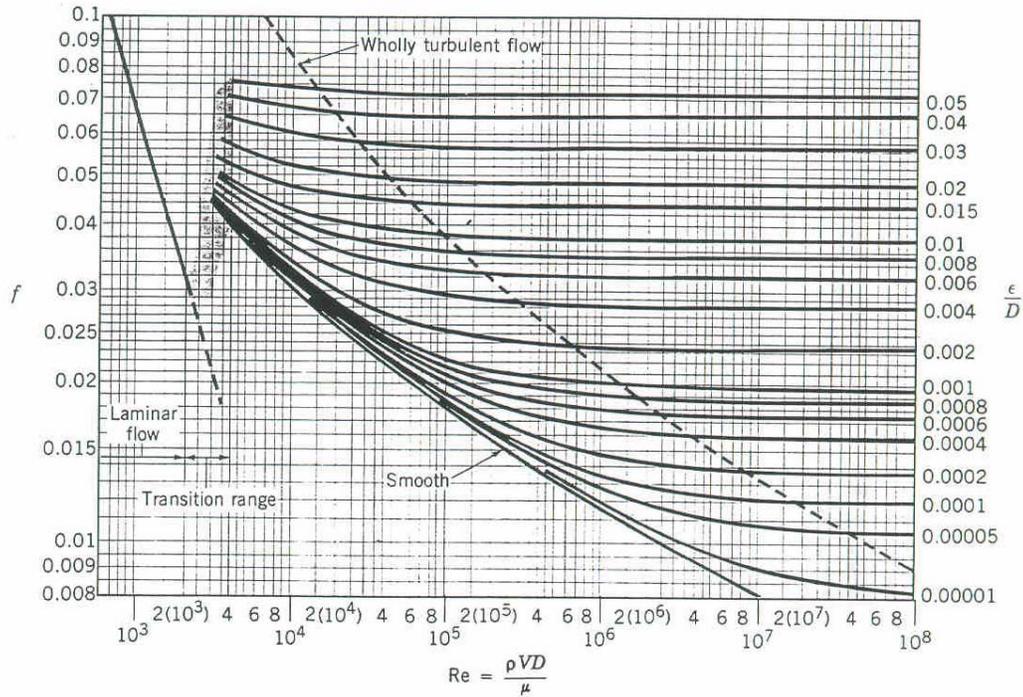
Figure 3.6. Moody Chart

The Moody Chart (Fig. 3.6.) was used to obtain f from the calculated Reynolds

number and ε/D. The Reynolds number was computed as vD/ν, where D was the pipe

diameter, v was the mean water velocity in the pipe, and ν was the kinematic viscosity of

water (10^{-6} m^2/sat 20° C). ε/D represents the pipe roughness where ε is the average

height of the roughness elements on the pipe surface, D is the pipe diameter and equals

4R, R equals the hydraulic radius, A/P, therefore D equals 4A/P which can be written as

2ab/(a+b) for a rectangular pipe, where a is the cross-sectional area of the pipe and b is

the pipe perimeter. Once the shear stress was calculated, an erosion vs. shear stress curve

was obtained for each test sample.

It should be noted that the SRICOS method for determining ε/D uses the roughness element, ε, equal to ½ of the D_{50} based on the assumption that only half the particle protrudes into the flow. However, it was decided that a more relevant roughness would be that of the pipe surface roughness, since the pipe walls constitute approximately 65% of the perimeter of the cross section compared to the soil sample that comprises approximately 35% of the perimeter of the same cross section. While this is a minor change causing no more than a 10% difference in f, it was judged to be more indicative of the roughness factors controlling turbulence in the pipe.

The critical shear stress for each layer of soil found at the site was determined as outlined above and this shear stress as well as the depth of the soil layer it came from, was entered into the soil data window of the SRICOS program (Figure 3.7).

Figure 3.7. Soil Data window, SRICOS (2004)

Briaud et al. (2003) determine the critical velocity and critical shear stress as those that correspond to the shear and velocity that produce 1mm of erosion. Since this method of determining the critical velocity may bracket the true critical velocity, another test was conducted on 4 of the 5 samples. This new experiment was performed to ascertain the actual critical velocity of the soil. The test used the same Shelby tube soil samples as above and the sample was prepared in the same manner; i.e. the Shelby tube was placed on the EFA piston and the sample was trimmed flush with the top of the tube. However prior to placing the tube flush to the flume bottom, a waterproof colored marker was used to place 9-10 dots on the top of the centerline of the soil sample, 5mm from the downstream end of the tube. The dots were placed in a straight line that was approximately 10mm in length. The area for the placement of the dots was chosen to avoid the small micro-eddies produced by the tube rim. The sample was placed flush to the bottom of the flume as before but this time the sample was not pushed into the flow. The initial velocity was kept constant and slow (approximately 0.5m/s). If no erosion of the dots occurred within one minute the velocity was increased and the dots were observed again. If after 1 minute no change in the dots was observed, the velocity was increased in the same manner until movement was observed. When the dots began to fade, the velocity was kept constant and the time to fully erode the dots was recorded along with the velocity. This procedure was repeated 8 to 9 times with velocities that bracketed the initial velocity where movement was observed to obtain a velocity curve from which the critical velocity could be determined. It was believed that this method gives a more accurate threshold shear for very small D_{50} material that could help extend and refine Neill's curves. (Figure 3.8.)
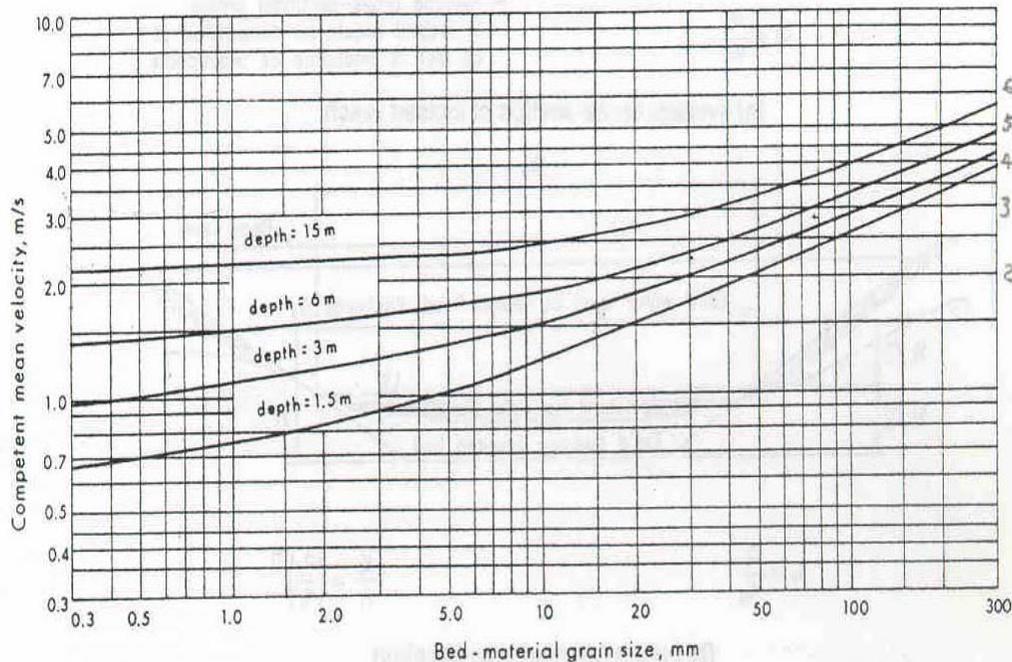
Figure 3.8. Neills Curves for Competent Velocities (TAC, 2001)

Neill's curves are one means of estimating critical velocities in fine materials such as sands and silts. They showed that small bed –material grain size eroded at small competent (critical) velocities and that large bed-material grain size eroded at high competent (critical) velocities in a straight-line relationship. Neill felt that there was some influence of fine materials on the resistance of soil for a D_{50} size below 0.3mm (fine sand), which is why his curves stop at that particle size.

3.4. Hydrograph Methodology

3.4.1. Generation of Synthetic Hydrographs for Ungaged Sites

Briaud (1999) used USGS stream gage data as input to SRICOS. A search of USGS gages found that there were gages on the stream of 4 of the 5 sites selected but 3

of these gages were of little value due to their distance from the bridge site. Since most

Maryland streams do not have gages at bridge sites, a method was developed by Dr. Kaye

Brubaker of the University of Maryland Civil Engineering Department to produce

synthetic hydrographs for the desired time period.

The synthetic hydrograph method was used to create several sequences of daily

stream discharge at four of the study sites: MD 7 at White Marsh Run, MD 26 at

Monocacy River, MD 28 at Seneca, and MD 355 at Great Seneca. The method was not

applied to the Woodrow Wilson bridge site, because it was not possible to analyze the

Potomac River with the Maryland GIS-Hydro 2000 (Moglen, 2000) tool (the Potomac

River basin extends beyond the boundaries of the state of Maryland). The White Marsh

site was collocated with a stream gage; therefore the statistics of observed flow were used

to determine the parameters for the streamflow generation routine. At the remaining three

sites, a regression equation was applied to determine the parameters

A 160-year hydrograph was decided upon as having the best chance of producing

large event stream flows. The entire method is provided in Appendix C at the back of

this report. The synthetic hydrographs were stored as text files for input to SRICOS.

3.4.2. Woodrow Wilson USGS Modified Hydrograph

The hydrograph used for the Woodrow Wilson Bridge site was based on the

USGS Little Falls gage upstream of the bridge. This gage accounted for all but 300 sq.

miles of the 11,860 sq. mi. watershed.   The gage data was adjusted to add this 300 sq.

mi. watershed to the total discharges. This was accomplished by first, pro-rating the

flows from downstream of the gage to the bridge for the 2-,5-,10-,25-,50-,100-, and 500-

year storms based on the unit runoff as measured in cfs. The first column of the table

Fig. 3.2 shows the developed discharges for the 2-, 5-, 10-, 25-, 50-, 100-, and 500-year storms at the gage site. (WW Br. Proj., 2000)

In order to apply a pro-rated Q to the Little Falls hydrograph a method to add pro-rated Q's to each discharge was needed. This was accomplished by graphing the design storm Q's from the gage vs. pro-rated Q's for these design storms. A linear regression was performed and an equation of the line was found. (Figure 3.9.)
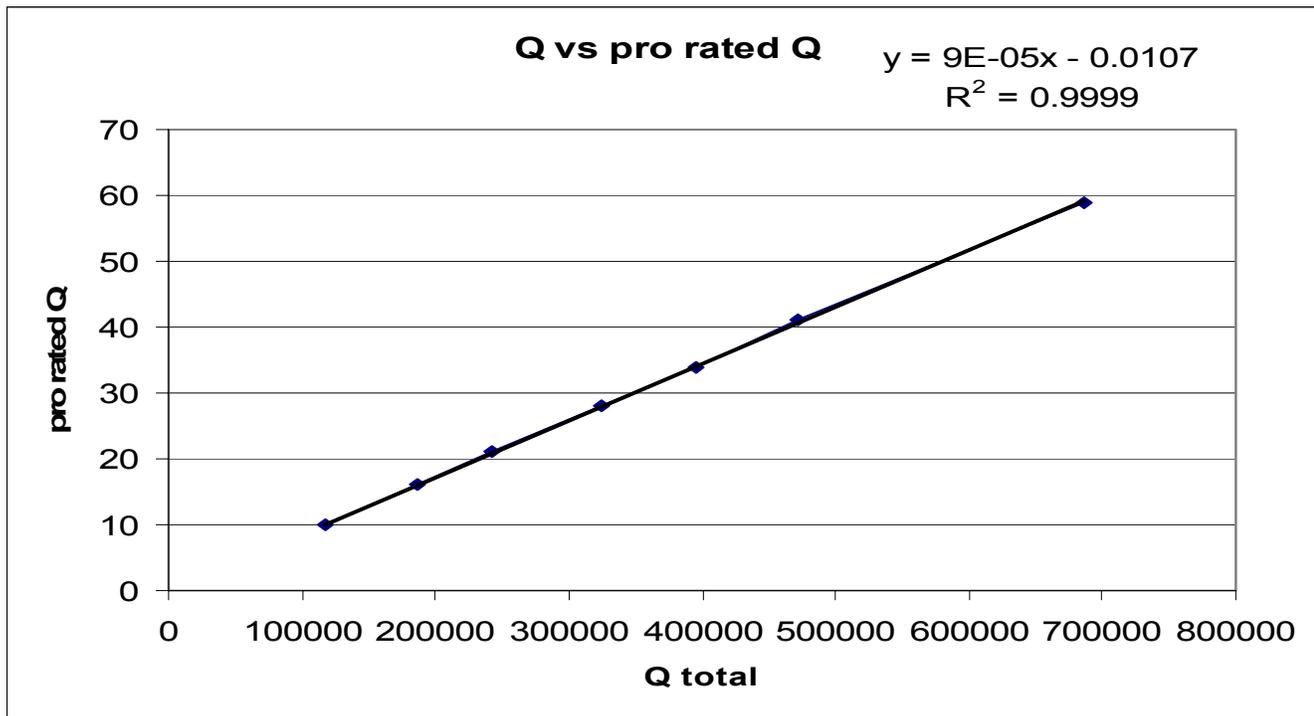
Figure 3.9. Discharge v. Pro-Rated Discharges for Added Watershed area, Woodrow Wilson Bridge

Table 3.2. Design Discharges for I-95 Bridge

Q	Pro rated Q report	Calculated pro-rated Q from eq.	Incremental Change (cfs)	Design Discharges (cfs)
117000	10	10.52	3156	120156
187000	16	16.82	5046	192046
243000	21	21.86	6558	249558
325000	28	29.24	8772	333772
395000	34	35.54	10662	405662
472000	41	42.47	12741	484741
687000	59	61.82	18546	705546

26

Column two of Table 3.2 shows the discharge per square mile of the added watershed in the WW Bridge report. Column three is the calculated pro-rated discharge from the equation of the line from Figure 3.8. Column three was multiplied by the area of the added watershed (300 sq. mi.) and this incremental change was added to the gage discharges to obtain the design discharges in column five, which were used as the SRICOS hydrograph for the Potomac River.

3.5. Converting Discharge to Velocity Hydrographs

A model of each bridge site was made in the hydraulic program HEC-RAS. HEC RAS is a hydraulic model developed by the ARMY Corps of Engineers' Hydrologic Engineering Center and is the most widely used hydraulic program for modeling riverine systems. HEC RAS allows the user to enter surveyed cross sections of the river, structure geometry, friction coefficients, ineffective flow areas, and other variables to obtain water surface elevations, energy elevations and - most importantly for this project - flow velocities for given discharges through the bridge cross section. HEC-RAS allows the user to specify up to 45 stream tubes at a given cross section to obtain data on specific areas of concern. Use of this option provided velocity data at the location in front of the piers (whether in the overbank area or the main channel) without the bridge and bridge piers, as specified by Briaud (1999). The reason given for modeling the site without the bridge in place is "removal of the piers is necessary because the velocity used for the pier scour calculations is the mean depth velocity at the pier location if the pier were not there." (Briaud etal. 2003)

A table was made of the velocity for a given discharge at the selected pier. Varying discharges were run through the hydraulic program to provide a curve of discharge vs. velocity and velocity vs. water depth in the overbank area where the pier is located. These tables are required input to the SRICOS program. The tables developed for the Maryland study differ from the original SRICOS method in that the piers in the Texas study were in the river channel and therefore had higher velocities associated with the discharges. The tables were entered into the water data window of the SRICOS program (Figure 3.10).

Figure 3.10. Water Data Window, SRICOS program (2004)

3.6. Predicting Bridge Pier Scour at Maryland Sites with SRICOS

Once all the hydraulic parameters have been acquired and the shear stress v. erosion as well as the hydrograph has been obtained the SRICOS program can be run. The program uses the following steps to calculate the maximum scour depth at a complex pier as outlined in the SRICOS manual.

The SRICOS program was originally developed to predict the scour depth versus time for circular piers in deep water at a constant velocity and a uniform soil. This equation was modified for complex piers with correction factors to account for shallow water depth, effect of rectangular shapes, angle of attack, and pier spacing. However, the method does not account for the effect of exposed footings at this time. SRICOS requires an erosion rate versus the hydraulic shear stress curve, obtained from the EFA tests. The maximum hydraulic shear stress (τ_{max}) around the pier is calculated first. The initial erosion rate corresponding to τ_{max} is read determine the erosion rate from the erosion rate curve that was developed empirically. The maximum shear stress for a given velocity is calculated as:

$$\tau_{max\ (pier)} = 0.094\ \rho\ v\ [(1/\log Re) - .1]\ K_w * K_{sp} * K_{sh} * K_a \qquad (3.2)$$

where: ρ = density of water

    v = average velocity at pier location (bridge not there)

    K_w = correction factor for water depth

        For H/B <= 1.6 $K_w = 0.85\ (H/B)^{0.034}$

        For H/B > 1.6 $K_w = 1$ H = water depth, B = pier width

    K_{sp} = correction factor for pier spacing

    K_{sh} = correction factor for shape, = B1 / (B1-nB)

K_a = correction factor for attack angle

Re   = Reynolds number, vB/v,

B = pier diameter,

v = kinematic viscosity of water

Note that the K correction factors in equation 3.2 account for some of the same corrections factors in the HEC-18 equation but the values of these K factors are different. HEC-18 also accounts for the bed condition and bed armoring that SRICOS does not and HEC-18 has supplemental correction factors for various pier conditions including very wide piers and complex pier foundations.

The next step is to calculate the maximum pier scour depth, z_{max} and constructing the erosion versus time curve from which the scour depth corresponding to the flood duration is read. Briaud developed the following equation empirically:

$$Z_{max(pier)} = .18 \ K_w * K_{sp} * K_{sh} * K_a * Re^{.635} \qquad\qquad (3.3)$$

The shape of the scour depth versus time curve is defined as:

$$Z = t / [(1/z_i) + (t/z_{max})] \qquad \text{t is in hours} \qquad\qquad (3.4)$$

This procedure describes scour depth associated with one velocity. However rivers have varying discharges and velocities over time. To accommodate these changing conditions the SRICOS researchers modified the procedure. The scour depth calculations choose the time increment as 24 hours and break the hydrograph into partial flood events each lasting 24 hours. Two velocities are handled by assigning the velocities as v_1 and v_2 and the times of the events as t_1 and t_2. The scour depth versus time curve for flood 1 is:

$$z_1 = t/[(1/z_{i1}) +(t/z_{max1})] \qquad\qquad (3.5)$$

And for flood 2 as:

$$z_2 = t/[(1/z_{i2}) +(t/z_{max2})] \qquad\qquad (3.6)$$

Flood 1 creates a scour depth z_1 that would have been created in a shorter time, t_e, by

flood 2 (if $v_2>v1$). This shorter time can found by the equation:

$$t_e = t_1/[(z_{i2} / z_{i1}) + t_1 z_{i2} (1/ z_{max1} -1/ z_{max2})] \qquad\qquad (3.7)$$

Flood 2 starts at a scour depth of z_1 which is the equivalent of having flood 2 for time t_e

to achieve the same scour depth. Scour is predicted for flood 1 according to the flow and

duration of that flood. Flood 2 will cause additional scour only if its flow and duration

are predicted to cause greater scour to occur. Only the additional scour is added to the

total scour prediction. The program advances by considering a new "flood 2" and a new

t_e at each new velocity. (Fig. 3.9.) The output of the program is the scour depth over the
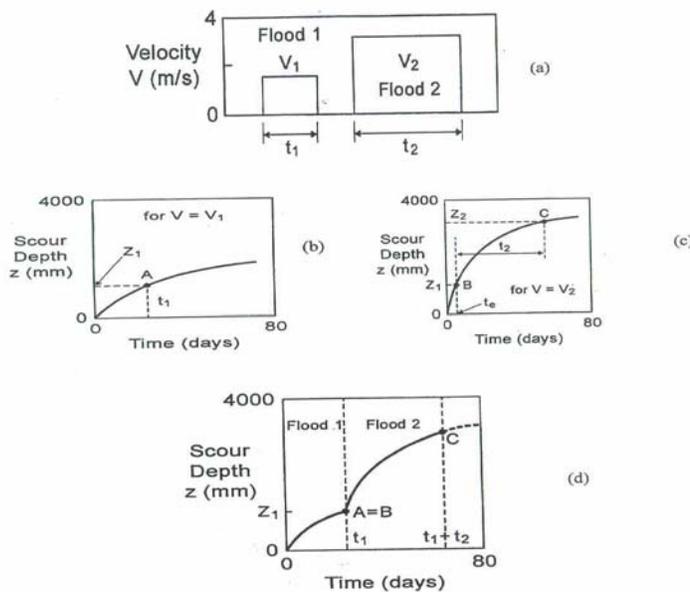
time of the hydrograph.

Figure 3.11. Scour Due to a Sequence of Two Floods (Courtesy of Briaud)

31

In the case of multi-layered soils when the scour depth enters a new soil layer, the computations follow the same process now using the new layer's erosion versus time curve and starting at the previous flood's final scour depth. The SRICOS code steps are outlined in the National Cooperative Highway Research Program (NCHRP) report 24-15.

SRICOS allows the user to insert a 100- and/or 500-year storm into the hydrograph at proscribed intervals. Since four of the synthetic hydrographs used in the SRICOS program did not show a 100-year storm, the SRICOS option of inserting the 100-year storm was used in all cases except. The MD 7 over White Marsh Run site contained a discharge larger than the 500-year storm. However, due to the geometry of the structure and the high tailwater, the 500-year storm had bridge velocities that were smaller than the 100-year discharge and so the 100-year storm was inserted into the hydrograph.

SRICOS converts the discharge hydrograph into a velocity hydrograph and provides a table of velocity, maximum scour depth and accumulated scour depth for all given discharges with a final scour depth reported for the last discharge entry on the hydrograph.

For comparison purposes the HEC-18 pier scour depth (described in Section 2.2) was also calculated. HEC-18 has become the standard method used by engineers to estimate maximum design pier scour. The equation, however, is designed for cohesionless soils and is independent of time. It is widely regarded as being a conservative estimate of scour in cohesive soils.

4.0 FINDINGS

4.1. Soil Characteristics and EFA Data

Shelby-tube boring samples were collected from each of the five study sites. The soil characteristics of each sample are listed in Table 4-1. The Erosion Function Tables for each tested Shelby tube are tabulated in Appendix A and are graphed as erosion rate versus shear stress in Figures 4.1 -4.10.

Three usable Shelby tube samples were collected at the White Marsh Run site all at a depth between 1' – 3'. These sample tubes were bored in the vicinity of the proposed bridge pier in the overbank area. The three tubes were all classified under the USCS soil classification system as sandy lean clay with D_{50} of 0.0234mm, 0.0530mm and 0.389mm respectively. The Atterberg Limits were also quite similar as can be seen in Table 4.1 and the plasticity chart shows soils of inorganic clays of low plasticity.

Two Shelby tubes were recovered from the Monocacy River site, which were classified by USCS as lean clay with sand. Again the Atterberg Limits of the two samples are quite similar and represent inorganic clays of medium plasticity on the plasticity chart while the D_{50} of the two samples are 0.0178mm and 0.0087mm.

Three Shelby tubes were collected at the Seneca Creek site and four analyses were performed. These samples had different soil classifications assigned to them. The first tube recovered at a depth of 5' to 7'was classified as silt and a D_{50} of 0.0114mm. The second tube recovered at a depth of 7' to 8.5' in the same boring hole as tube 1 was classified as lean clay with sand with a D_{50} of 0.0178. The third tube recovered at a depth of between 5' and 7'was classified as silt with sand and had a D_{50} of 0.0328mm in

Table 4.1. Comparison T=Soil Table of Shelby Tubes

| | | | | | | | | | % Retained | Threshold | Threshold | |
Site	Boring	Sample	D50 (mm)	Gravel Content, %	Sand Content, %	Silt Content, %	Clay Content, %	on #200 Sieve	Shear (lbs/ft^2)	velocity (ft/s)	clay/sand
MD 28	B-3	Tube 1, 5'-7'	0.0178	7.6	15.4	51.1	25.9	23	0.141	5.58	1.68
		Tube 2, 7'-8.5'	0.0114	0	4.2	67.8	28	4.2	0.074	3.87	6.67
	B-3A	5'-7', 1st analysis	0.0328	0	29.8	50.3	19.9	29.8	0.050	3.25	0.67
		5'-7', 2nd analysis	0.0358	0	26.5	55.3	18.2	26.5	0.030	0.74	0.69
MD 26	B-1	Tube 1, 4'-6'	0.0074	2.8	5.7	52.9	38.6	8.5	0.074	4.04	6.77
		Tube 2, 6'-8'	0.0087	0	19.2	43.7	37.1	9.3	0.112	5.15	1.93
Md 355	B-2	Tube 1, 2'-4'	0.0243	6.8	17.1	55.5	20.6	33.9	0.151	5.97	1.20
		Tube 2, 6.5'-8.5'	0.0442	5.9	30.3	40.8	23	36.2	0.153	5.97	0.76
MD 7	B-3	Tube 1, 1'-3'	0.0234	3.7	35.1	32.3	28.9	38.8	0.100	4.92	0.82
	B-2A	Tube 2, 1'-3'	0.053	8.8	37	27	25.2	47.8	0.07	3.94	0.68
	B-2	Tube 3, 1'-3'	0.0389	6.5	39	27.3	27.2	45.5	0.26	7.48	0.70
WW Br	B-8	72-73'		16.3	1.2	7.1	75.4	17.5	0.0215	2.00	62.83
WW Br.	B-3	58-60'	0.308	2.8	85	7	5.2	87.8	0.02	1.64	0.06

Comparison Table of Soil Characteristics

the first analysis that represented the first 12 inches of soil recovered. During the EFA

testing of the next 12 inches of tube 3, it became apparent that another type of soil layer

had been uncovered. This soil was analyzed separately for soil characteristics and

classified as lean clay with sand and it had a D_{50} of 0.0358mm.

The two tubes recovered from the Great Seneca Creek site over MD 355 were

collected from the same boring hole at 2' to 4' for tube 1 and 6.5' – 8.5' for tube 2. The

soil of tube 1 was classified as lean clay with sand and had a D_{50} of 0.0243mm. The soil

of tube 2 was classified as sandy lean clay with a D_{50} of 0.0442mm.

Finally, because the Woodrow Wilson Bridge is one of the busiest interstate

bridges in the country, retrieval of Shelby tubes from the bridge was not possible.   In

addition the cost of using a river barge to retrieve the tubes was prohibitive. After careful

analysis of the known soil layers under the bridge, the same soil layers were located by

MSHA geotechnical engineers on the Maryland shore at a depth of 58'-60' for tube 1 and

a depth of 72' to 73' for tube 2. Tube 1 had a D_{50} of 0.308 and a soil classification of

silty sand. Tube 2 had a D_{50} that was too small to ascertain. 81.7% of the soil was finer

than #270 sieve; however the D_{85} was 2.24mm and a soil classification of clay with 84%

of the soil being clay, 14% silt and 2% sand.

The Woodrow Wilson Bridge Shelby tubes presented some problems. The first

Shelby tube taken at a depth of 58'-60' was found to have dent in the middle of the tube.

This prevented the EFA piston from pushing the sample and required stopping the tests

before a full EFA test of the material could be performed as can be seen by table 4.1.

The second Shelby tube taken at a depth of 72' contained very stiff clay that was too stiff

for the motor of the piston to push. This test was also terminated and no results were possible.

The erosion rate curves for each EFA tested site were developed. (Figures 4.6 through 4.12) The EFA measures the velocity and erosion in m/s and mm/hr. The equation for shear stress ($\tau = 1/8\ f\rho v^2$) was used to obtain the erosion rate v. shear stress curves. The shear stress was then converted to English units (lbs/ft^2) as were all other units except for the erosion, which SRICOS requires to be entered in the metric units, for ease of use with previous studies.
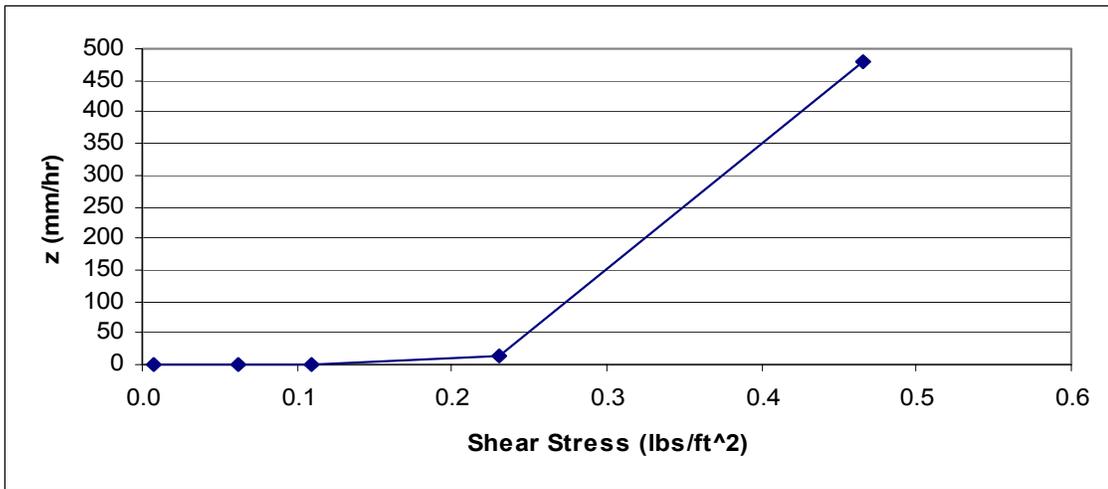

Figure 4.1. Erosion Rate Curve, MD 26 over Monocacy River, Tube 1
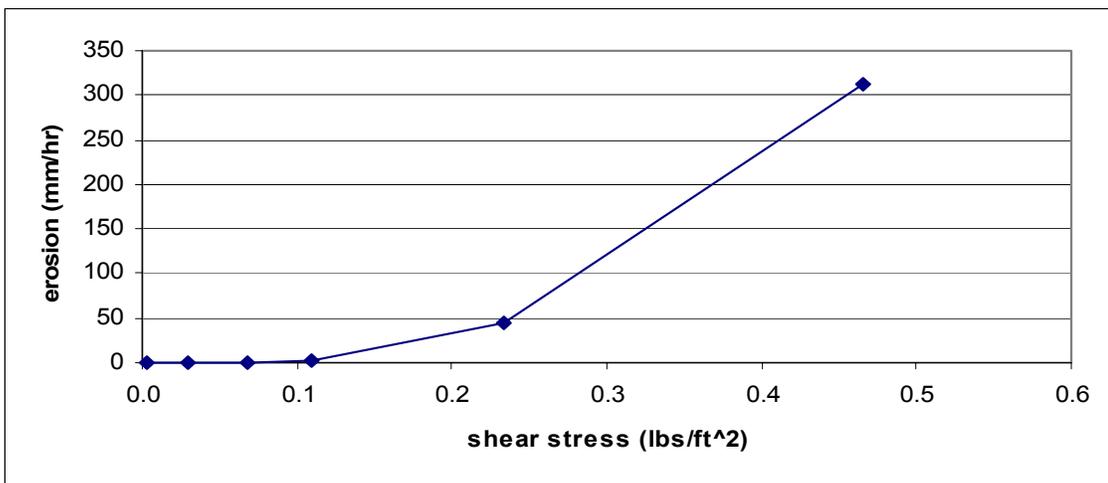

Figure 4.2. Erosion Rate Curve, MD 26 over Monocacy River, Tube 2

Figure 4.3. Erosion Rate Curve, MD 355 over Great Seneca Creek, tube 1, 2'-4'
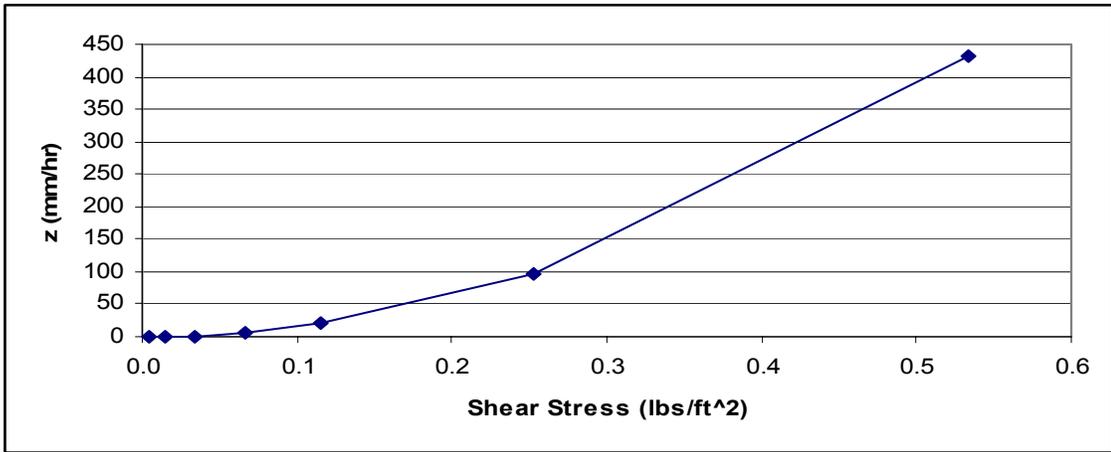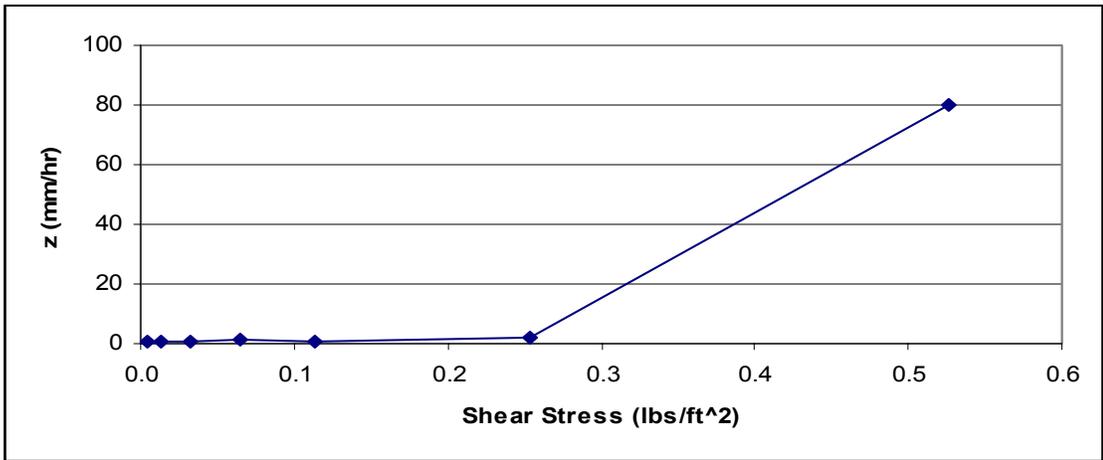

Figure 4.4. Erosion Rate Curve, MD 355 over Great Seneca Creek, Tube 2, 6'-8'

Figure 4.5. Erosion Rate Curve, MD 28 over Seneca Creek, Tube B-3A, 5'-7'

37

Figure 4.6. Erosion Rate Curve, MD 28 over Seneca Creek, Tube B-3, 5'-7'
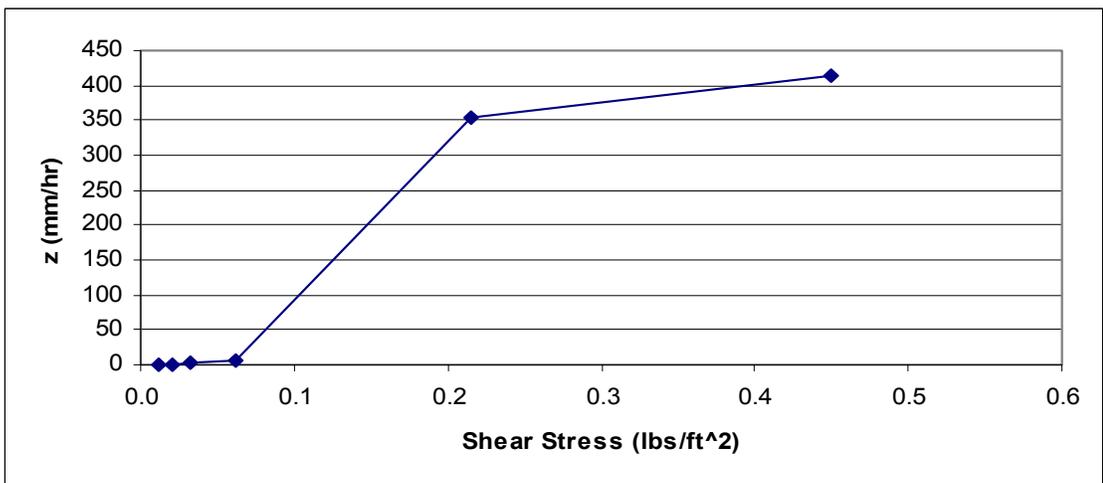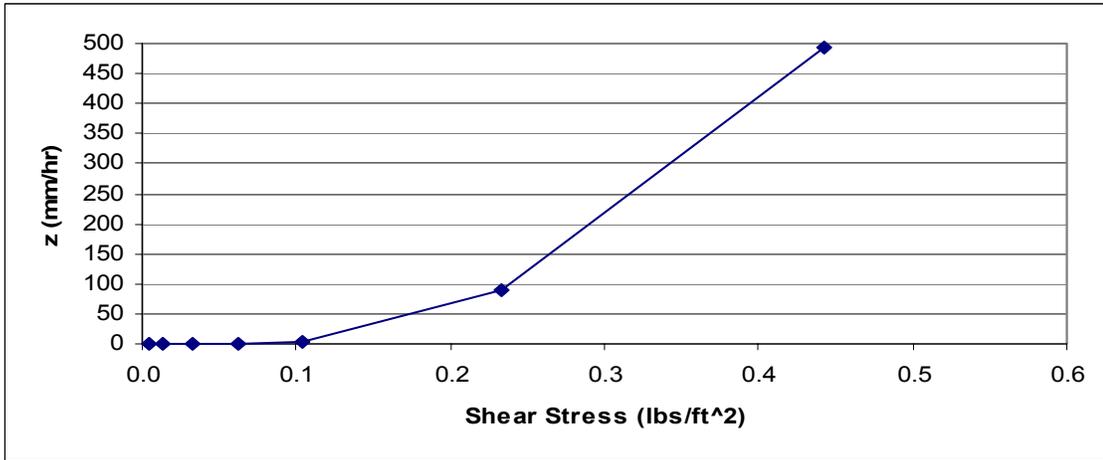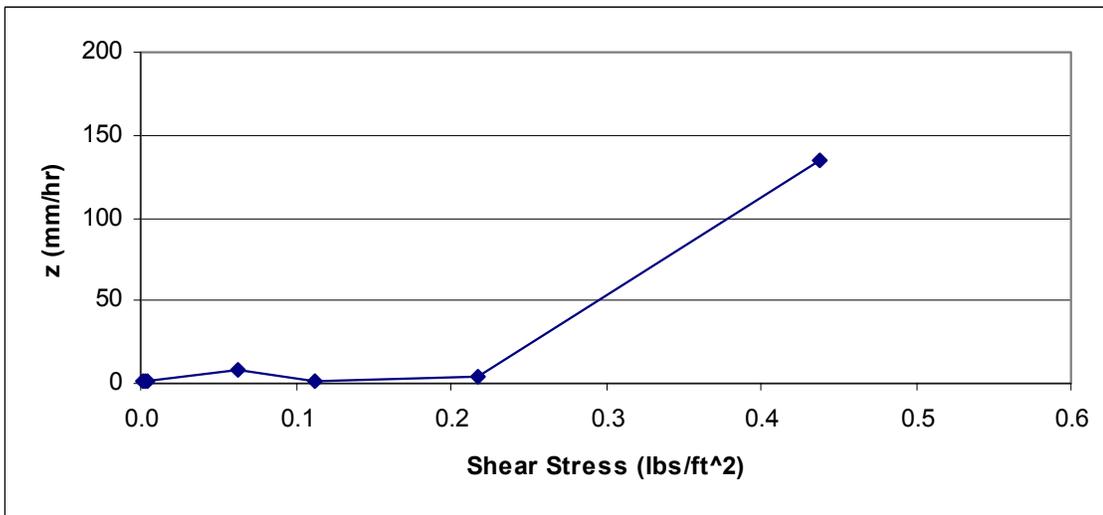

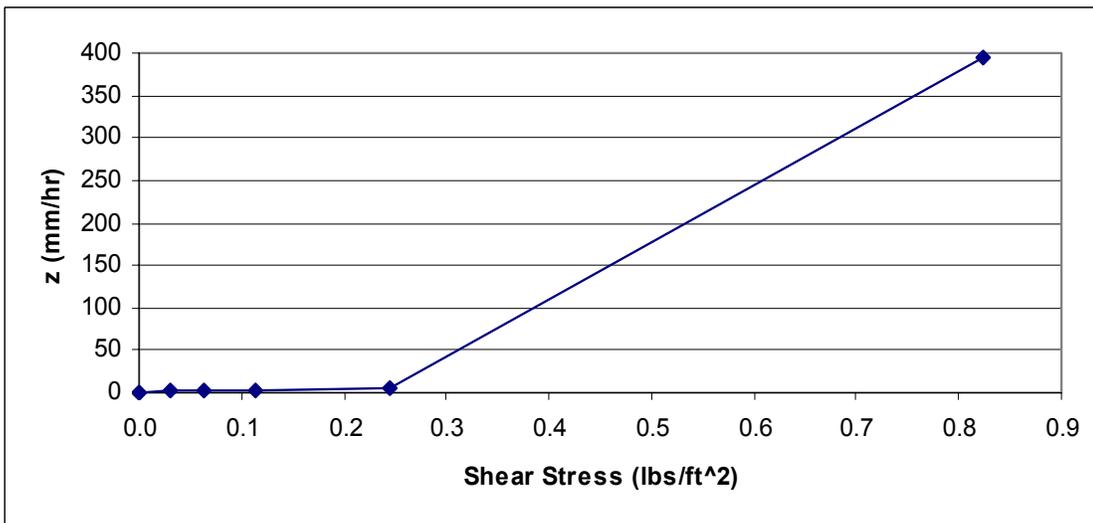Figure 4.7. Erosion Rate Curve, MD 28 over Seneca Creek, Tube B-3, 7'-8.5'

Figure 4.8. Erosion Rate Curve, MD 7 over White Marsh Run, Tube 1, 1'-3'
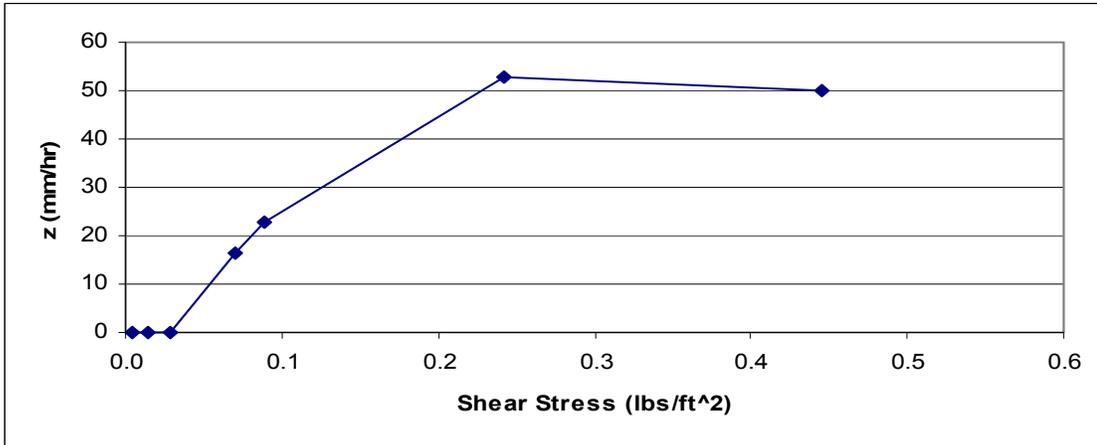
Figure 4.9. Erosion Rate Curve,MD 7 over White Marsh Run, Tube 2, 1'-3'
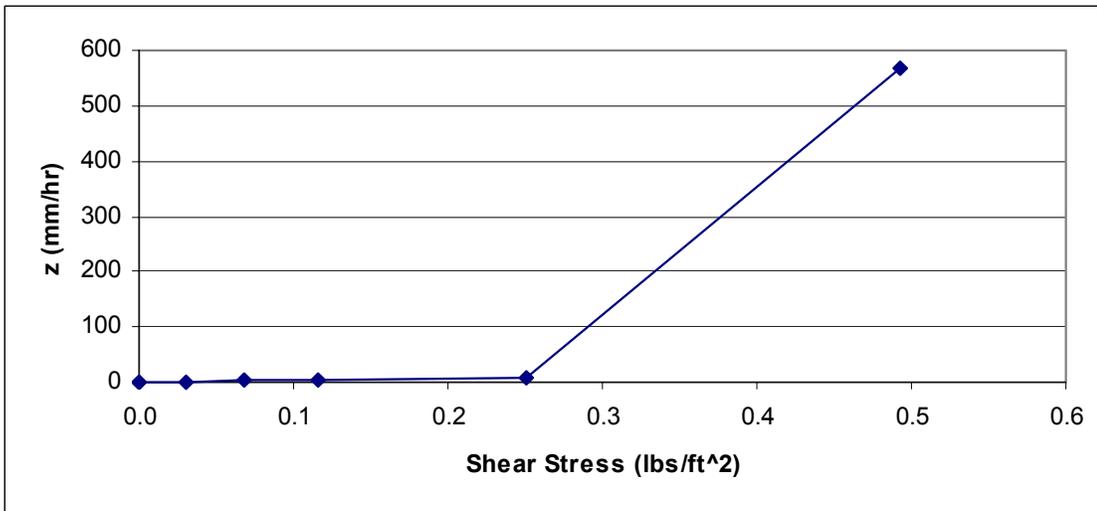
Figure 4.10. Erosion Rate Curve, MD 7 over White Marsh Run, Tube 3, 1'-3'
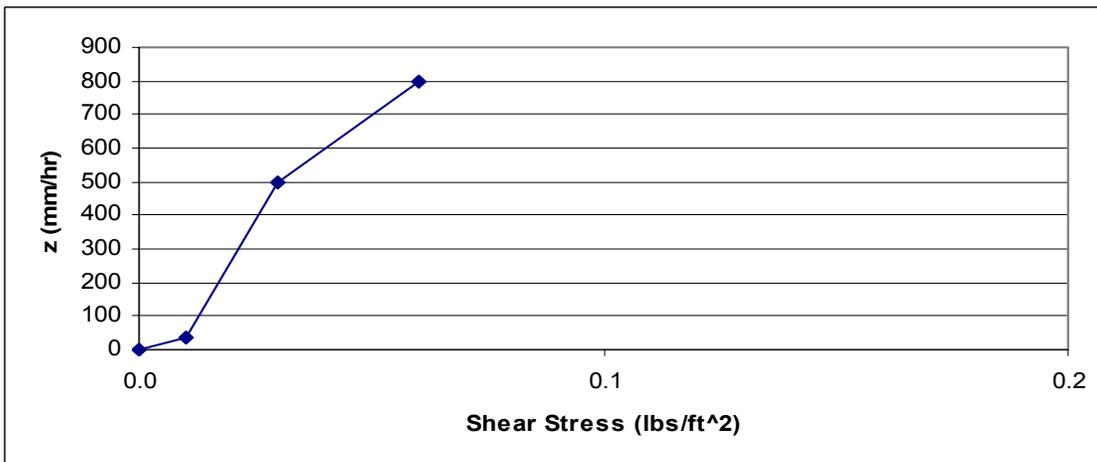
Figure 4.11. Erosion Rate Curve, MD 495 over Potomac River, Tube 58'-60'

4.2. Streamflow Generation

All the daily-discharge hydrographs for the four synthetically generated streamflows had the same time duration of 160 years. Table 4.2. below shows the 100- and 500-year instantaneous discharge estimates generated by GIS-HYDRO 2000 for each of the sites. Of the synthetic hydrographs generated, only the White Marsh Run site had a daily-discharge flow of 11,740 cfs that was greater than the 500-year storm. None of the four sites had a daily-discharge flow equal to the 100-year storm. Consequently, the 100-year flood event was inserted manually into the SRICOS program at all four sites to ensure that the worst case scenario was analyzed and for HEC-18 comparison purposes.

Table 4.2. Flow Characteristics

Site	Time (yrs)	100-year Peak Flow* (cfs)	500-Year Peak Flow* (cfs)
White Marsh Run	160	6300	10700
Monocacy River	160	81600	138700
Great Seneca Creek	160	17400	29580
Seneca Creek	160	30470	51800

*Instantaneous Peak Flow

The Potomac River hydrograph as explained in Chapter 3.4.2. was a modified USGS daily-discharge hydrograph of 80-year duration. Estimations of the 100-year and 500-year peak flows are 480,000 cfs and 575,000 cfs respectively (FHWA, 2000). The Potomac River hydrograph included a daily discharge of 465,000 cfs that was quite close to the 100-year instantaneous peak event of 480,000 cfs therefore, no flood events were inserted into SRICOS for this site.

4.3. Hydraulic Models

The five selected sites have all undergone extensive hydraulic analysis in preparation for replacement or added bridges. Although the SRICOS method suggests using only a few cross sections depicting the stream topography immediately upstream and downstream of the bridge as well as the bridge crossing itself, hydraulic models were used that encompassed stream profiles 1000-2000ft. upstream and downstream of the bridge. These stream profiles prove to generate more accurate estimates of flow velocities and water surface elevations in the vicinity of the bridge. The HEC-RAS models used for this study were based on the previous hydraulic models prepared for the new bridges.

Two of the models, MD 26 over the Monocacy River and MD 28 over Seneca Creek, were originally developed in HEC-2 and were converted into HEC-RAS. In accordance with the SRICOS method, the bridge geometry was removed from all the models but the roads, road embankments, and ineffective areas were left intact. Cross sections were placed at the toe of slope to provide velocity readings upstream of the piers.

The discharges run through the models included the 2-, 10-, 25-, 50-, 100-, and 500-year design storms. Unlike the Texas bridge piers, where the piers are found in the main channel, Maryland bridge piers are placed outside the main channel in an effort to minimize stream degradation in the vicinity of the bridge. With the use of the stream tube option in HEC-RAS, it was possible to ascertain the flow velocity immediately upstream of the pier. The velocity/water depths of this study reflect flows that reach the piers whether they are in the overbank or in the main channel. Consequently, the flow

discharge may be large, but the velocity on the overbank at the location of the pier may be much lower than in the main channel.

4.4. Pier Scour Estimates

The scour estimates presented were based on the synthetic hydrographs. Only MD 7 over White Marsh Run's hydrograph included the 500-year storm discharge. To better estimate the possible scour at the pier, the 100-year design storm was inserted into the hydrograph as an option within the SRICOS program. The following SRICOS scour estimates are based on these hydrographs with the 100-year storm inserted. The SRICOS scour estimates are shown in Table 4.3.

As expected, the calculations of the HEC-18 scour equations show more conservative scour estimates than the SRICOS estimates. (Table 4.3.) All HEC-18 calculations relied upon the data generated by the proposed models with the bridge in place; the standard procedure used for HEC-RAS.

Figures 4-12 through 4-16 show the SRICOS scour results. If only one flood is manually inserted into the hydrograph, SRICOS places it midway through the hydrograph. Four of the five selected sites had the 100-year discharge inserted into their hydrographs and it is apparent from the figures that this discharge causes the most scour. The White Marsh Run hydrograph included a storm greater than the 500-year storm But that storm led to more overtopping and had lower velocities than the 100-year storm. As a result Figure 4.12 shows that the 100-year discharge for White Marsh Run causes much of the scour at the pier. I-95 over the Potomac River, Figure 4.16 that used the adjusted USGS 80-year hydrograph shows scour caused by several large events other than the 100-year discharge, which all contribute to the pier scour. Figure 4.15 of MD 28 over

Seneca Creek shows that even the 100-year discharge produces only 0.2 ft of scour; a very small scour depth due to the large bridge length (500'+) and the low flow velocities in the overbank area. The pier of the Monocacy River Bridge sits out of the daily base flow but it is subjected to larger flows. Figure 4.13 shows approximately 3 feet of scour that jumps to approximately 8 feet of scour produced by the 100-year inserted discharge. Scour at the Great Seneca Creek bridge pier, Figure 4.14, also shows that the 100-year inserted storm was the cause of all scour at this bridge.

Table 4.3. Comparison of scour depths

Site	SRICOS Scour (ft)	HEC-18 Scour (ft)
MD 7 over White Marsh Run	3.2	5.4
MD 28 over Seneca Creek	0.2	8.4
MD 355 over Great Seneca Creek	2.3	4
MD 26 over Monocacy River	7.7	12.4
Woodrow Wilson Br.	26.5 (incomplete)	30-46
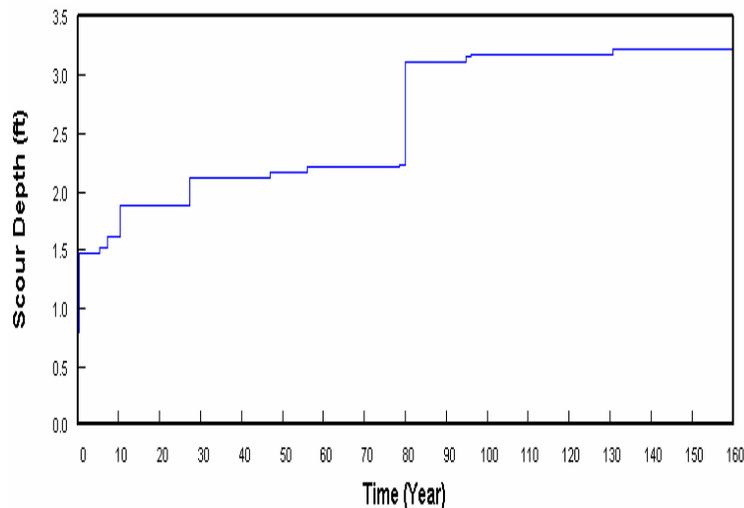
Figure 4.12. SRICOS Scour Results, White Marsh Run
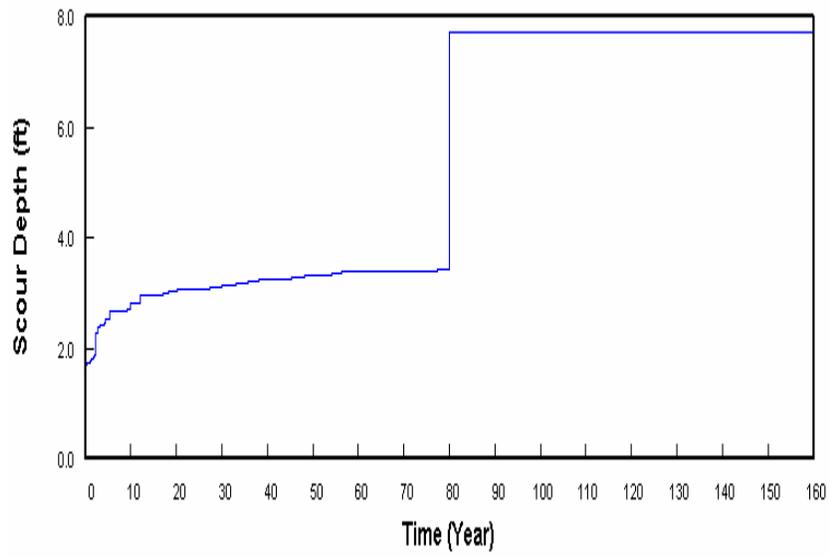
Figure 4.13. SRICOS Scour Results, Monocacy River
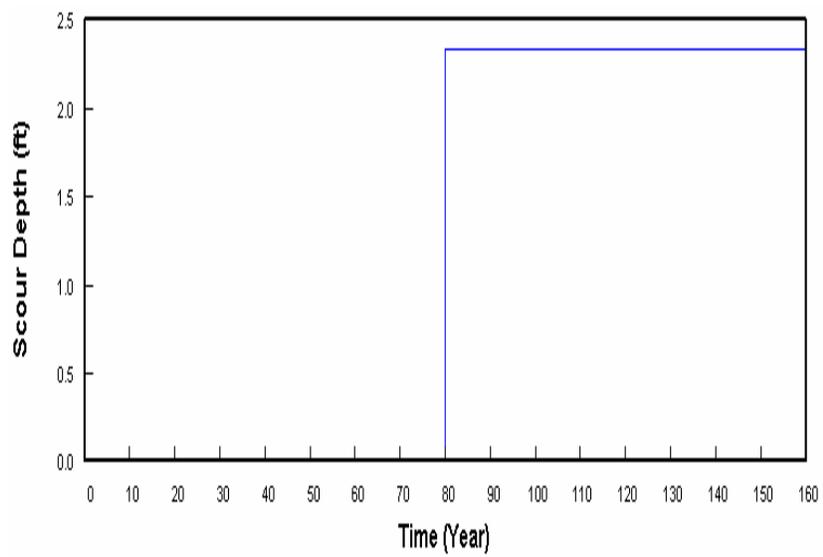
Figure 4.14. SRICOS Scour Results, Great Seneca Creek
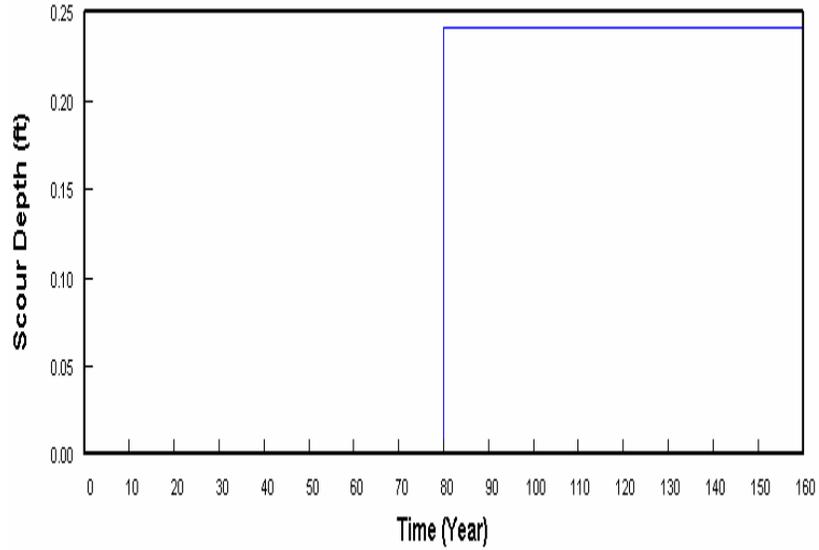
Figure 4.15. SRICOS Scour Results, Seneca Creek
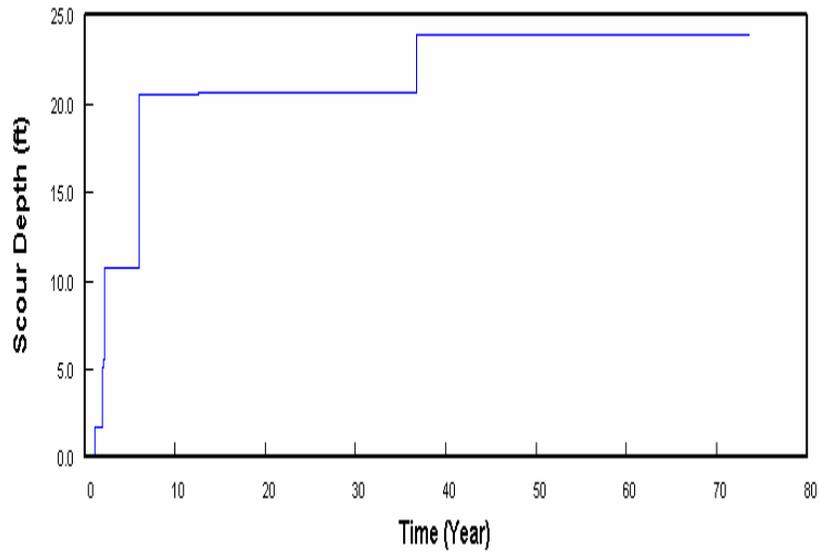
Figure 4.16. SRICOS Scour Results, Potomac River

Although the SRICOS scour depths are less than the HEC-18 scour depths, it is Maryland State Highway Administration policy to predict a minimum of 5 feet of scour at bridge structures. As can be seen by Table 4.3, three of the five selected sites have SRICOS scour depths that are less than five feet. Consequently these scour depths would

45

be increased to the minimum five feet canceling out any benefit of running EFA/SRICOS calculations at these sites.

The Woodrow Wilson Bridge site had comparable scour depths although the SRICOS scour depths are not complete due to mechanical problems encountered with the soil samples.

4.5. Discharge Order

The MSHA study of which this thesis was a part devoted substantial effort to a method to create realistic discharge hydrographs. In examining the results, the question was raised, how important is the order of discharges in the SRICOS scour calculation? The following investigation was conducted to explore that question.

Big Flood – Little Flood
Md 26 over Monocacy River
Flood 1

Q = 81600	cfs	K_w =	1	
H = 10.23	m	K_{sp} =	1	
Vel = 1.97	m/s	K_{sh} =	1.1	
ρ= 1000	kg/m^3	K_a =	1	
$\acute{\alpha}$= 0		time =	24	hrs
v= 0.000001		B =	1.83	m

Re = vel B/v = 3605100

$$\tau = .094*\rho*vel^2(1/\log Re - .1)*K_w*K_{sp}*K_{sh}*K_a = .094*1000*1.97\text{^}2(1/\log 3605100-.1)*1.1$$
$$= 21.07 \quad \text{N/m\text{^}2}$$
$$\text{from } Z_i \text{ curve at 21.07 N/m}^2 \text{ } \tau_{max} = 430 \quad \text{mm/hr}$$

$$Z_{pier\,max} = 0.18*K_w*K_{sp}*K_{sh}*K_a*Re^{.635} = .18*1.1*3605100\text{^}.635$$
$$= 2886 \quad \text{mm}$$
$$z_1(t) = t/((1/z_i)+(t/z_{max1})) = 24/((1/430)+(24/2886))$$
$$= 2255 \quad \text{mm}$$
$$= \boxed{7.40 \quad \text{ft}}$$

Flood 2

Q = 36600	cfs		Kw =	1		
H = 7.28	m		Ksp =	1		
Vel = 1.67	m/s		Ksh =	1.1		
ρ= 1000	kg/m^3		Ka =	1		
ά= 0			time =	24	hrs	
v= 0.000001			B =	1.83	m	
= vel B/v = 3056100						

$\tau = .094*\rho*vel^2(1/\log Re - .1)*K_w*K_{sp}*K_{sh}*K_a =$ .094*1000*1.67^2*(1/log3056100 -.1)*1.1

$\qquad\qquad\qquad\qquad\qquad\qquad\qquad\qquad$ = 15.63   N/m^2

$\qquad$ from Z_i curve at 15.63 N/m^2 τ_{max} = 210   mm/hr

$Z_{pier\,max} = 0.18*K_w*K_{sp}*K_{sh}*K_a*Re^{.635} =$ .18*1.1*3056100^.635

$\qquad\qquad\qquad\qquad\qquad\qquad\qquad\qquad$ = 2599   mm

$t_e = t_1/((z_{i2}/z_{i1})+t_1*z_{i2}(1/z_{max1}-1/z_{max2})\ )=$ 24/((430/210)+(24*430)(1/2886)-(1/2599))

$\qquad\qquad\qquad\qquad\qquad\qquad\qquad\qquad$ = 81.3   hrs.

$\qquad z_2(t) = t_e+t_2/((1/z_{i2}\ )+(t_e+t_2/z_{max2})) =$ 81.3+24/((1/210)+(81.3+24/2599))

$\qquad\qquad\qquad\qquad\qquad\qquad\qquad\qquad$ = 2325   mm

$\qquad\qquad\qquad\qquad\qquad\qquad\qquad\qquad$ = **7.6**   **ft**

The SRICOS program predicted a scour depth of 7.74 ft.

Another scenario of little flood followed by a big flood was also performed.
Little Flood – Big Flood
 Flood 1

Q= 36600	cfs		Kw =	1		
H = 7.28	m		Ksp =	1		
Vel = 1.67	m/s		Ksh =	1.1		
rho = 1000	kg/m^3		Ka =	1		
alpha = 0			time =	24	hrs	
nu = 0.000001			B =	1.83	m	

$\qquad\qquad\qquad$ Re = vel B/v = 1.67*1.83/.000001

$\qquad\qquad\qquad\qquad\qquad\qquad$ = 3056100

$\tau = .094*\rho*vel^2(1/\log Re - .1)*K_w*K_{sp}*K_{sh}*K_a =$ .094*1.67^2*(1/log3056100-.1)*1.1

$\qquad\qquad\qquad\qquad\qquad\qquad\qquad$ = 15.63   N/m^2

$\qquad$ from Z_i curve at 15.63 N/m^2 τ_{max} = 210   mm/hr

$Z_{pier\,max} = 0.18*K_w*K_{sp}*K_{sh}*K_a*Re^{.635} =$ .18*1.1*3056100^.635

$\qquad\qquad\qquad\qquad\qquad\qquad\qquad$ = 2599   mm

$\qquad\qquad z1(t) = t/((1/zi)+(t/zmax1)) =$ 24/((1/210)+(24/2599))

$\qquad\qquad\qquad\qquad\qquad\qquad\qquad$ = 1715   mm

$\qquad\qquad\qquad\qquad\qquad\qquad\qquad$ **5.63**   **ft**

Flood 2

Q = 81600	cfs	Kw =	1	
H = 10.23	m	Ksp =	1	
Vel = 1.97	m/s	Ksh =	1.1	
rho = 1000	kg/m^3	Ka =	1	
alpha = 0		time =	24	hrs
nu = 0.000001		B =	1.83	m

$$Re = vel \ B/v = \ 3605100$$

$$\tau = .094 * \rho * vel^2 (1/\log Re - .1) * K_w * K_{sp} * K_{sh} * K_a = \quad 21.07 \ N/m^2$$

from Z_i curve at 21.07 N/m^2 $\tau_{max} =$ 430 mm/hr

$Z_{pier \ max} = 0.18 * K_w * K_{sp} * K_{sh} * K_a * Re^{.635} =$ 2886 mm

$t_e = t_1/((z_{i2}/z_{i1}) + t_1 * z_{i2}(1/z_{max1} - 1/z_{max2})) = 24/((430/210) + 24 * 430(1/2599 + 1/2886))$

2.5 hrs.

$z_2(t) = t_e + t_2/((1/z_{i2}) + (t_e + t_2/z_{max2})) =$ 2303 mm

7.6 ft

The SRICOS program predicted a scour depth of 7.74 ft.

The order of these two events does not make a difference. SRICOS predicted 7.7ft. of scour for 160 years of record. This means that although smaller storms do cause some scour it is a minimal amount and the large storms cause the majority of the scour at the pier.

4.6. Investigation of Hydrograph Assumptions

The synthetic streamflow method attempts to capture the statistics of daily discharge, whereas the 100-yr (Q100) discharge estimated by GIS-Hydro and used in design is an instantaneous peak flow, which has different statistical distributions. Peak flows generally last for a short time, and the corresponding daily average flow would be considerably smaller. One would not expect the daily-discharge simulation to produce flows as large as the instantaneous Q100. However, since MSHA design procedure dictates the use of instantaneous peak flows, the instantaneous Q100 was inserted into the

daily-flow hydrographs using the SRICOS option and was treated as if it lasted for 24 hours. The question was raised, what is the effect on scour if the instantaneous peak discharge is assumed to last for 24 hours, rather than a more realistic duration? This section describes an exercise to investigate the effects of this assumption on scour due to an event that includes the 500-year instantaneous peak.

SRICOS allows short-term event simulation using a shorter time step. Starting from the estimated instantaneous Q500, two different event hydrograph models were applied. These event hydrographs were run through the SRICOS program and the total event scour was analyzed. This scour was compared to the predicted scour that would result from a variety of averaging assumptions as described below.

A preliminary analysis of scour depths resulting from eight hydrographs made of 15 minute data entries based on different hydrographic assumptions was performed. MD 26 over the Monocacy River was selected as the test site. The hydrographs were based on the 500-year peak discharge and the underlying assumption for each hydrograph is described below per Dr. Brubaker:

Table 4.4. Hydrograph Assumptions

A	Dillow 1998	
B	Dillow Event Peak Event Duration	The peak discharge is assumed to apply for the duration of the entire event
C	Dillow Event Mean Event Duration	The event average is assumed to apply for the duration of the entire event
D	Dillow 24-hr Peaks 24 Hr Each	The event is split into 24-hr periods, and the peak flow within each 24-hr period is assumed to apply for that period
E	Dillow 24-hr. Means 24-hr each storm	The event is split into 24-hour periods, and the average flow over each 24-hour period is assumed to apply for that period (This is what the daily Q record would show if this event actually occurred, starting at midnight)
F	SCS Event	
G	SCS Event Mean Event Duration	The event average is assumed to apply for the duration of the entire event
H	Peak 24 Hr	The peak discharge is assumed to apply for 24 hours (This is what we get when the Q peak is "inserted" into the hydrograph for SRICOS)

49

SRICOS produced the following scour depths resulting from the hydrographs:

Table 4.5. Maximum Scour Depths

Hydrograph	Maximum Scour Depth (ft)
A	7.82
B	N/A
C	7.82
D	7.82
E	7.95
F	7.95
G	8.2
H	8.42

As can be seen the maximum scour depths are dependent on the assumptions that form the basis of the hydrograph model. Hydrograph B that assumed the peak event lasted 24 hours could not be run due to an unexplained error in SRICOS. The 24-hour peak event, hydrograph H, produced the largest scour depths however; this hydrograph does not represent a typical storm event.

It is not the intent of this study to determine the best assumptions to be used in modeling hydrographs for scour studies but rather to show how assumptions can affect the predicted maximum scour depths. It is recommended that more study and research be implemented in the future to determine the best hydrograph model to use.

4.7. Results of Critical Velocity Tests

The critical velocity test results are shown in Fig 4.18. as part of Neill's chart of critical velocity of sandy soils as a function of water depth, velocity and flow depth. (TAC, 2001) The dots on the left of the chart represent the critical velocity (competent velocity on chart) of the cohesive soil samples. If Neill's curves were extrapolated to grain sites characteristic of clays, one would expect cohesive soils to have a critical velocity that is less than 1 ft/sec. It is unclear where Neill's data came from but Chang (2003) theorizes after comparing the Fortier – Scobey western canal velocities to Neill

Curves that the Fortier – Scobey data is the basis of the curves. The Fortier – Scobey

velocities were taken in open channels whereas the critical velocity tests performed for

this study were done in a closed conduit flowing full. The closed conduit was only 2

inches high but it also had a head produced by the water pump that contributed somewhat

to the increased critical velocities of the cohesive soils tests. The chart reveals that the

cohesive soils have critical velocities in the 3 to 6 ft/sec range. Because these clay soils

do not have the same composition it is difficult if not impossible to make generalizations

about the results. What the experiment gives promise to is if similar types of clay are

tested over many samples, it may be possible to make equivalent Neill's Curves for

cohesive soils for use as a reference for scour calculations. More experiments of these

cohesive soils were out of the scope of this study but it presents some interesting

possibilities that could prove useful to cohesive scour computations in the future.
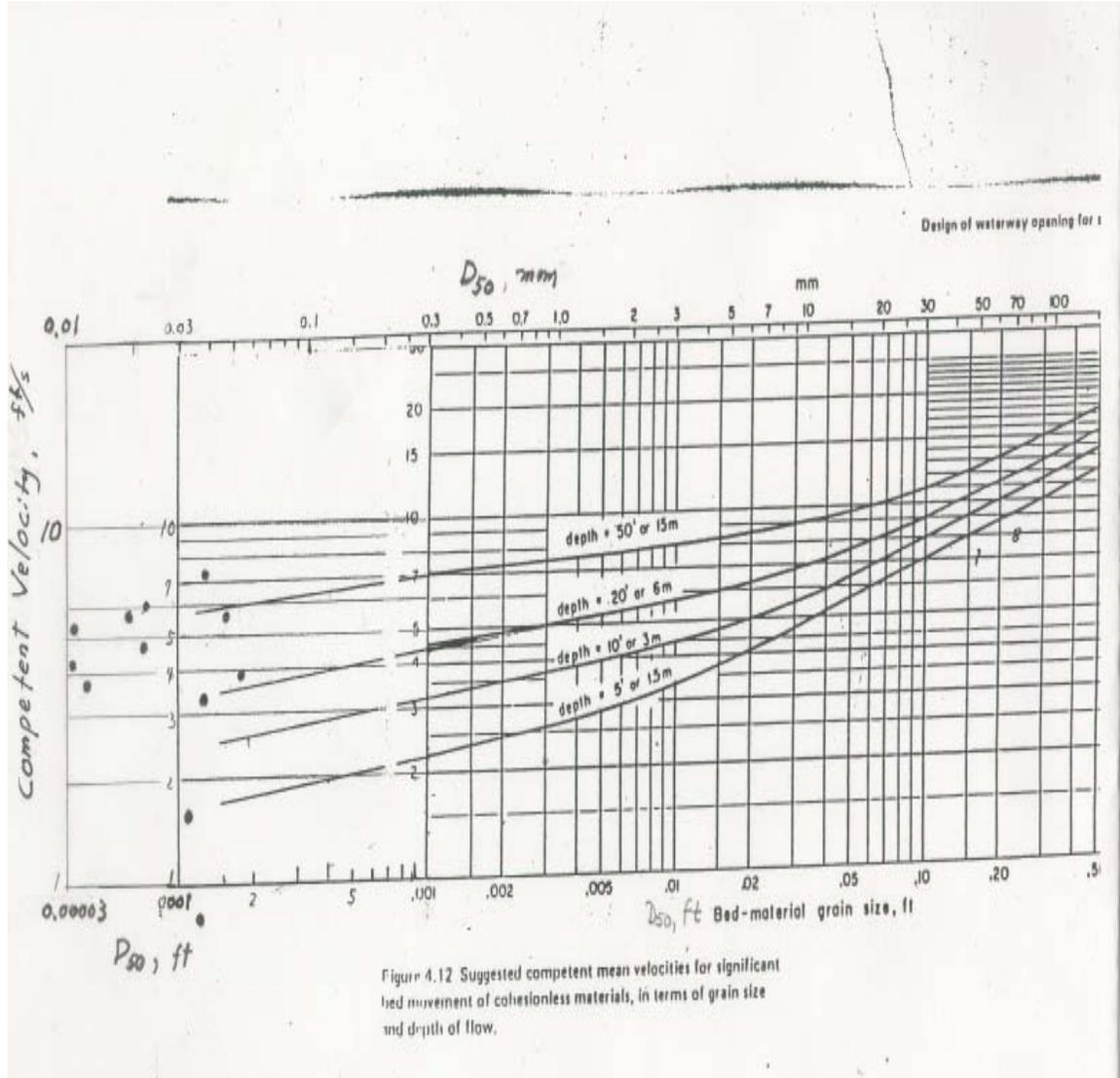
Figure 4.12 Suggested competent mean velocities for significant bed movement of cohesionless materials, in terms of grain size and depth of flow.

Figure 4.17. Neill's Curve extended

5. DISCUSSION

5.1. Assessment of EFA and SRICOS techniques

5.1.1. EFA Erosion Modeling

Soil in a riverbed acts a porous, semi-rigid boundary. The soil particles resist horizontal movement due to shear stress of water flowing over them, and resist vertical movement that arises from water pressures building up in pores within the soil bed, below the particles.   The principle resistance to movement in cohesionless soil is by particle self-weight and by interlocking between adjacent particles in the soil bed. In the case of cohesive soils, other physical factors come into play that bind particles into larger units which usually results in greater resistance to erosion. Details of those units, including frequency and orientation of cracks, and mineralogy of the soil, both in situ as well as the representativeness of soil in the Shelby tube samples, will be important in characterizing erodibility of soil. Physical tests of erosion are certainly warranted, and the EFA is a step toward developing such a test. The following comments are made in the spirit of issues to consider in improvement of the EFA.

The EFA/SRICOS method predicts erosion of soils in riverbeds, assuming that flow is parallel to the soil surface. Once scour begins, however, the flow near the bottom of a scour hole moves in both vertical and horizontal directions, rather than in the straight flow seen in the EFA flume. This flow condition leads to more aggressive erosion behavior, because the dynamic pressure is greater and the pore pressure within the voids below the particles is increased. The particles move upward into the stream bed when the pore pressure is greater than the weight of the particles. Vertical components of velocity are found at the bottom of a pier and it is likely that this velocity is key to particle

movement in pier scour holes. The EFA flow conditions are, arguably, unconservative because it applies flow parallel to the soil surface and does not account for vertical components of erosive flow. Improvement in this regard is recommended.

In its implementation, the EFA presented some difficulties in obtaining satisfactory erosion rates. First, the proscribed method of pushing the sample 1mm into the streamflow introduces eddies around the sample that may cause scouring that is not caused by only the flow velocity.

Another difficulty is related to the difficulty of keeping 1mm of the sample in the streamflow. Not only is this difficult to assess, the fact that scour was rarely even across the sample surface meant that the decision of when to advance the soil became problematic. In one case, for example, a portion of a sample eroded more than 10mm on one side while another portion of the same sample remained unaffected by erosion. This led to uneven flow regardless of whether the soil was advanced.

The time to advance the soil also became a concern when testing at high velocities. The computer controlled push of the EFA piston led to a lag time of 1-2 seconds before the push occurred. At slow velocities this was not a matter of concern, however at higher velocities this lag produced erosion rates that were slower than what was actually seen. These slower rates then underestimate the amount of scour for a given velocity on the hydrograph.

After erosion commenced, the opacity of the water became an issue. The dirty water that quickly developed made observation of the sample difficult. The use of filters and possibly an automated method of determining when to push the sample could prove useful and improve repeatability.

Finally, characterizing erosion by conducting an erosion test on a real soil sample that includes natural layering and other non-uniformities, will be flawed because soil at different depths in the sample is likely to have different resistance to erosion.

5.1.2 SRICOS Modeling

There are two components of the SRICOS scour prediction program. First the soil characteristics of layer thickness and the shear stress at the proscribed EFA velocities and second the stream hydrograph with a user determined length. Both of these components pose some challenges.

The EFA erosion rates and computed shear stress from the experimental results are the foundation of the SRICOS scour analysis. As noted above in 5.1.1. the erosion rates are unconservative due to the lag time involved in pushing the sample soil. In addition these erosion rates do not account for the vertical components of velocity that occur at piers. The predicted scour depths reflect the inadequacies of the experimental method.

Whether using the standard USGS stream hydrographs or generating synthetic hydrographs, there is still debate about what are the best hydrographs for the intended purpose as noted in Chapter 4.6. Using the USGS average daily flow as the basis for the hydrograph is not conducive to capturing the high peak flows of large storm events. These high flood flows do most of the scouring at a structure but generally last only a few hours in even the largest watershed. By using the average daily flow these peak flows are averaged out and the effects from these peak flows are missed in the scour computations. The synthetic flow hydrographs used for this study recreated the same average daily flows following the concept used by Briaud etal. The watersheds that the hydrographs

are based on normally exhibit daily discharges that are relatively low base flows. This means that for any given day, a base flow or a slightly larger flow is more likely to be generated by the program than a large flood event. Therefore even when large numbers of hydrographs are generated, it is likely that no large discharges may appear. The result is hydrographs that may be underestimating maximum scour depths.

Although SRICOS allows the user to insert the 100- and 500-year flood events into the hydrograph, there is an incongruity of inserting what are instantaneous peak flows into a hydrograph of daily discharges.

5.2. Discussion of Results

5.2.1. EFA Conclusions

The EFA results are imperfect estimates of erosion rates in cohesive soils. They do not account for the vertical components of velocity at a pier; this will make results unconservative. The natural layering and non-uniformity of the soil can lead to under or over estimation of the rate of erosion. The mechanical difficulties of pushing the sample into the streamflow caused delays that can also make results unconservative. However, the EFA does provide a method of determining erosion rates from actual soil samples that was not possible before.

5.2.2 SRICOS Conclusions

The SRICOS method may be better suited to bridge piers in the channel as opposed to the overbanks as studied here. When the HEC-18 predicted scour depths were compared to the SRICOS predicted scour depths, SRICOS does show a significant reduction in predicted scour depths in four of the five sites as seen in Table 4.3 even with a hydrograph of 160 years duration. However, given the conservative MSHA policy of

estimating at least 5 feet of scour at a pier, the predicted scour depths at three of the sites would be raised to the minimum 5 feet of scour. The notion of a time dependent scour prediction model is enormously intriguing. The EFA/ SRICOS method may be used for the time being as another factor to consider in scour prediction but not the sole basis of the scour prediction. It is appropriate and understandable that designs that lead to less conservative assumptions of scour depth will require verification of those predictive methods, including field results if feasible. Verification of currently used methods are limited and tentatively suggest that HEC-18 scour prediction are conservative. If the mechanical difficulties of using the EFA can be overcome, if reasonable hydrograph assumptions can be determined, and if soil characteristics can be incorporated into the method then the EFA and possibly SRICOS may have the potential of becoming an accepted design scour prediction.

6. APPENDIX

APPENDIX A

EFA Data Reductions

Tables of Erosion Rates, Velocity and Shear Stress

from EFA tests of Sample Soils

MD 26, Tube 1, 4'-6'

vel(ft/s)	erosion (mm/hr)	shear (lbs/ft^2)
1.08	1.003	0.007
3.67	1.001	0.062
4.99	1.501	0.109
7.51	13.630	0.230
11.12	481.283	0.465

MD 28, Tube B-3A, 5'-7'

v (ft/s)	erosion (mm/hr)	shear (lbs/ft^2)
1.48	1.00	0.012
1.97	1.03	0.021
2.53	1.61	0.032
3.68	6.02	0.062
7.28	353.42	0.215
10.93	412.84	0.449

.
MD 26, Tube 2, 6'-8'

v (ft/s)	erosion (mm/hr)	shear (lbs/ft^2)
0.68	1.00	0.003
2.44	1.00	0.030
3.84	1.01	0.067
4.98	2.02	0.109
7.58	44.51	0.234
11.22	311.30	0.465

MD28, Tube B-3, 5'-7'

v (ft/s)	erosion (mm/hr)	shear (lbs/ft^2)
0.85	0.0	0.005
1.58	0.0	0.014
2.53	0.0	0.032
3.68	1.5	0.062
4.89	4.5	0.104
7.61	88.2	0.233
10.96	493.2	0.443

MD 355, Tube 2'-4'

v (ft/s)	erosion (mm/hr)	shear (lbs/ft^2)
0.75	0.00	0.004
1.54	0.00	0.014
2.46	1.00	0.034
3.67	5.52	0.067
4.95	21.61	0.116
7.41	96.67	0.253
11.06	430.62	0.534

MD 28, Tube B-3, 7'-8.5'

v (ft/s)	erosion (mm/hr)	shear (lbs/ft^2)
0.76	1.000	0.004
1.57	1.000	0.001
2.49	1.000	0.003
3.68	8.004	0.062
5.12	1.003	0.113
7.48	4.043	0.218
10.96	135.135	0.438

MD 355, 6.5'-8.5'

v (ft/s)	erosion (mm/hr)	shear (lbs/ft^2)
0.23	1.000	0.004
0.45	1.000	0.013
0.76	1.000	0.032
1.15	1.516	0.065
1.52	0.999	0.114
2.28	2.011	0.254
3.35	79.717	0.527

MD 7, Tube ,1 1'-3'

v (ft/s)	erosion (mm/hr)	shear (lbs/ft^2)
0.76	0	0.000
1.31	0	0.000
2.53	1.5	0.032
3.74	2	0.064
4.92	3.5	0.114
7.48	4.5	0.244
11.02	394.7	0.823

Woodrow Wilson 58'-60'

v (ft/s)	erosion (mm/hr)	shear (lbs/ft^2)
0.82	0	0.00
1.44	36	0.01
2.56	497	0.03
3.71	800	0.06

MD 7 Tube 2, 1'-3'

v (ft/s)	erosion (mm/hr)	shear (lbs/ft^2)
1.0	0	0.005
1.6	0	0.014
2.3	0	0.028
3.94	16.5	0.070
4.59	23	0.089
7.87	52.63	0.242
11.16	50	0.446

MD 7 Tube 3, 1'-3'

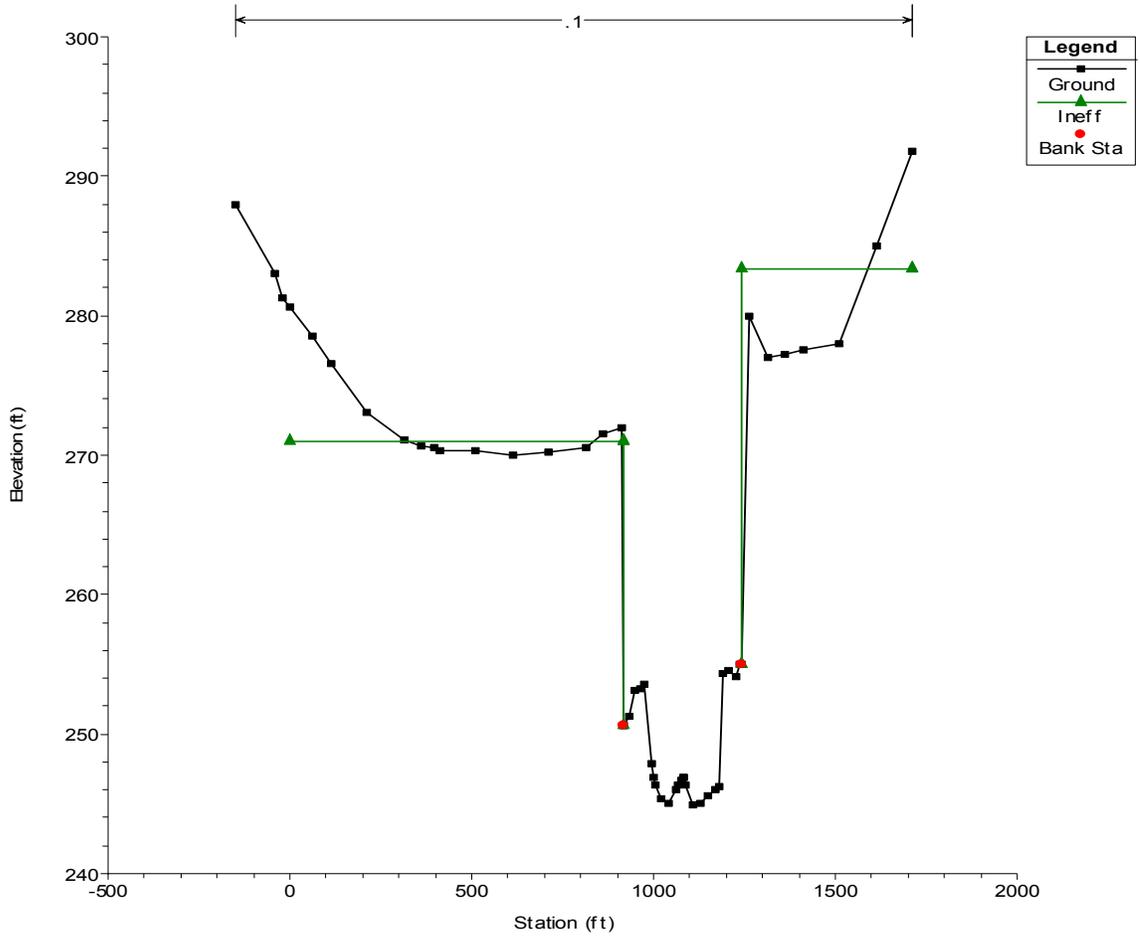| v (ft/s)	erosion (mm/hr)	
0.89	0	0.0
1.47	0	0.0
2.43	2	0.030
3.87	3	0.068
5.05	3.0	0.116
7.58	6.5	0.251
11.45	566.0	0.493

APPENDIX B

HEC-RAS Analysis

MD 26 over Monocacy River

Upstream Bridge Cross Section

MD 26 over Monocacy River, vol 2 of 2

Q	Velocity (ft/s)	Water Depth (ft)
200	0	0
500	0.92	0.58
1000	1.52	1.72
5000	2.61	7.97
10000	3.02	12.98
19500	3.83	18.81
36600	5.49	23.89
67200	6.35	30.85
81600	6.46	33.57
138700	6.76	40.92

MD 28 over Seneca Creek

Upstream Bridge Cross Section
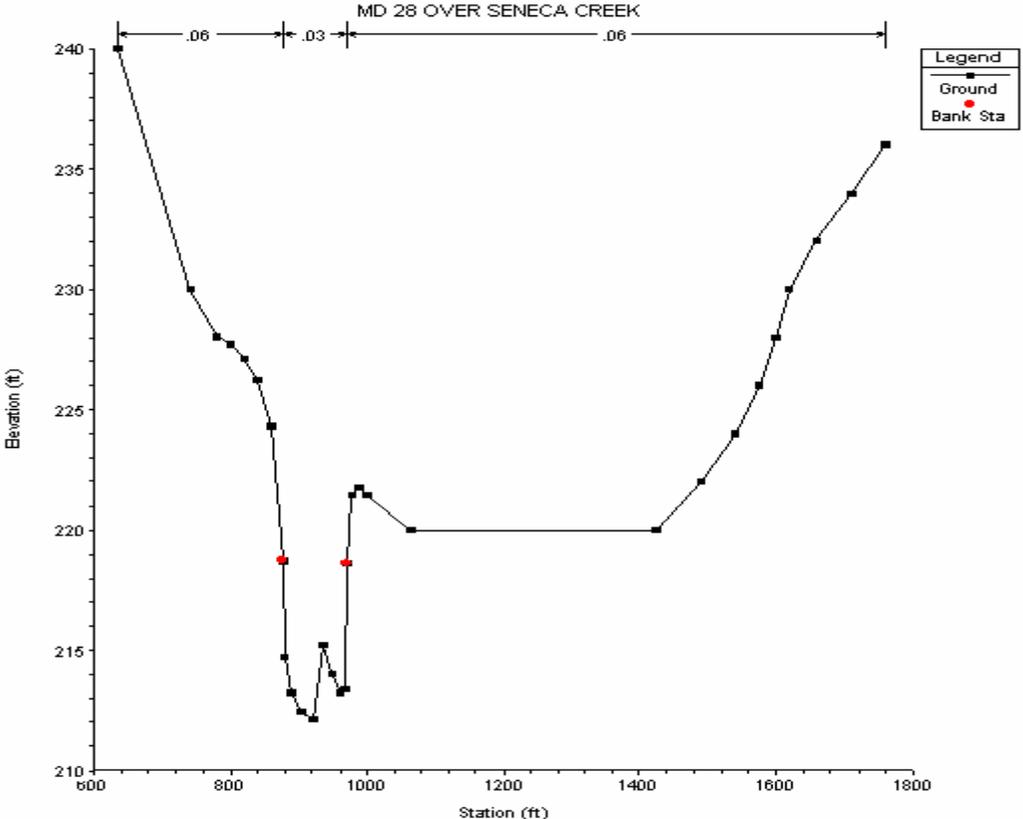
Q	Velocity (ft/s)	Water Depth (ft)
2950	0.04	0.02
5098	0.56	1
8960	1.19	2.73
9462	1.25	2.92
11600	1.49	3.67
14535	1.77	4.59
30470	2.48	10.07
51799	2.57	17.94

MD 355 over Great Seneca Creek

Upstream Bridge Cross Section
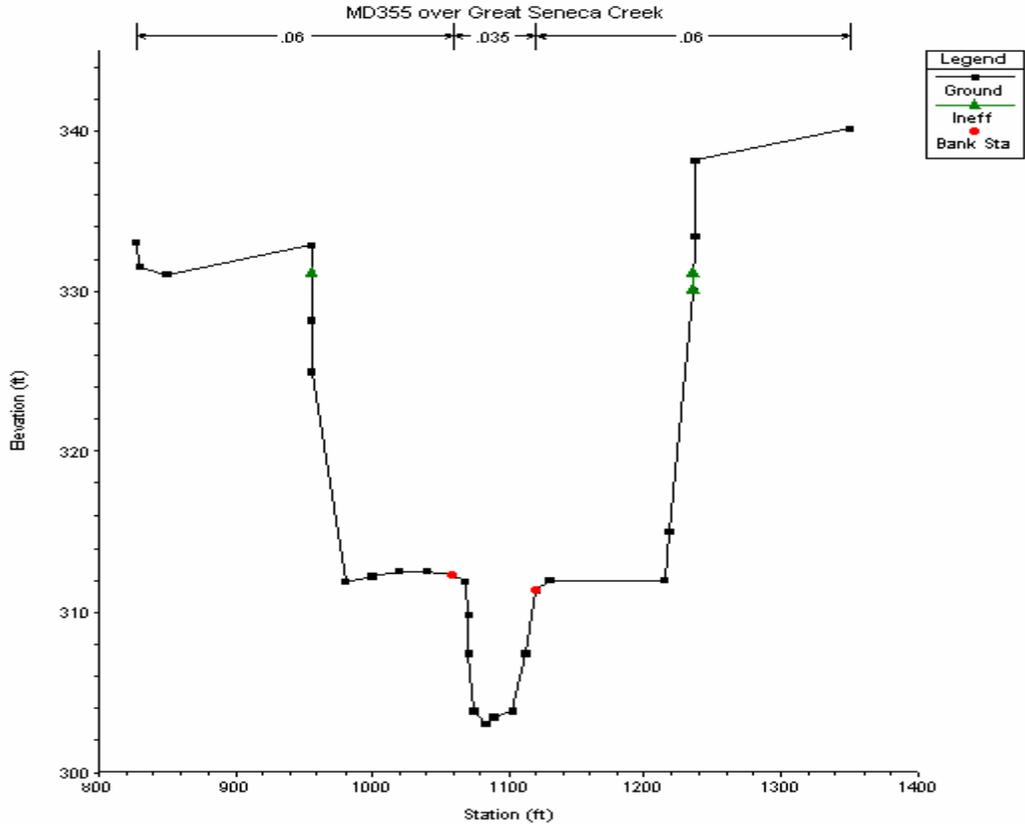
Q	Velocity (ft/s)	Water Depth (ft)
1000	0	0
1500	0.56	0.81
2000	1.13	2.06
3470	1.53	3.04
7600	2.56	6.31
10600	3.02	8.37
17400	3.65	12.73
29580	4.33	19.48

MD 7 over White Marsh Run

Upstream Bridge Cross Section

White Marsh Run, MD 7 to Rte. 40
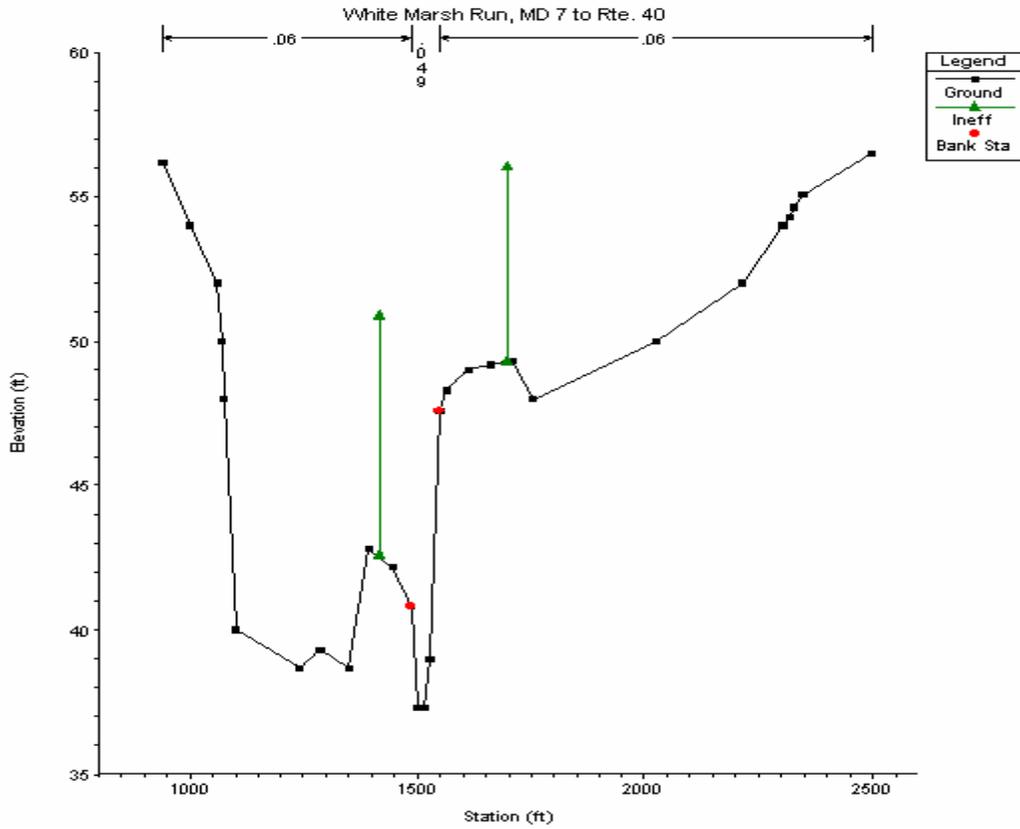
Q	Velocity (ft/s)	Water Depth (ft)
500	0.8	0.69
800	1.2	1.29
1880	2.6	4.37
4540	4.08	7.51
5300	3.99	7.44
6300	4.05	8.57
7500	1.07	11.69
8500	1.16	12.32
10700	1.36	13.48
12000	1.19	14.29

I-95 over Potomac River

Woodrow Wilson Bridge

Upstream Bridge Cross Section
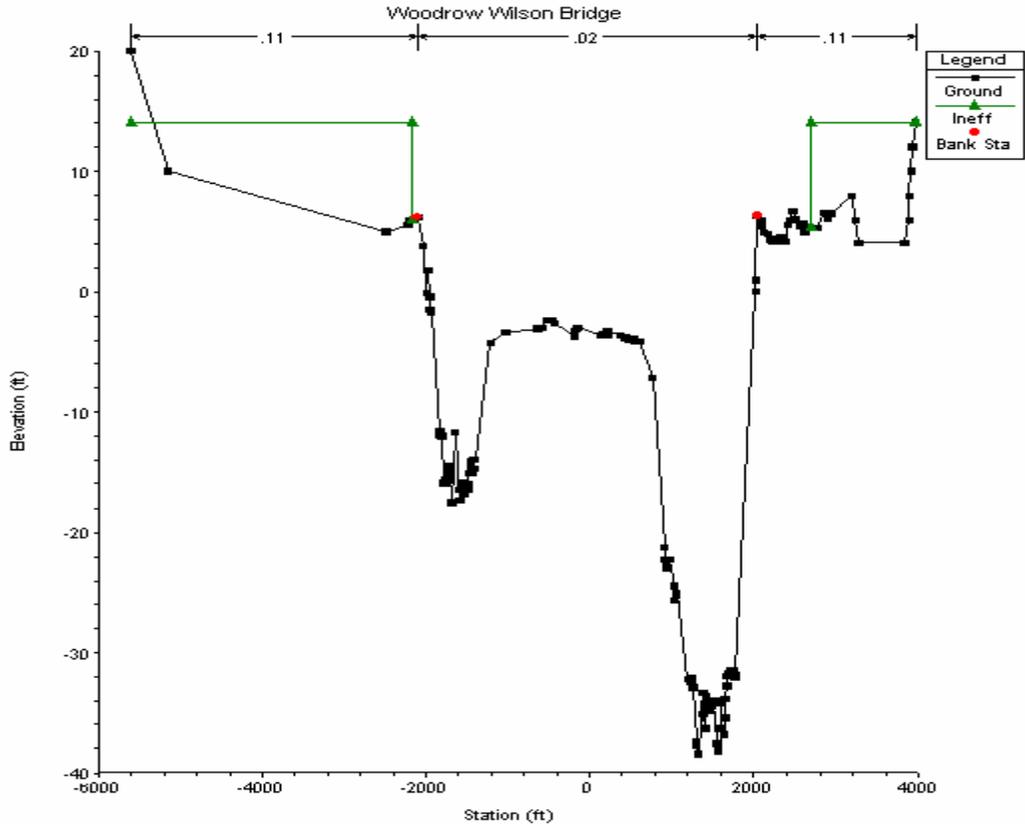
Q	Velocity (ft/s)	Water Depth (ft)
20000	0.22	11.95
120000	1.3	12.96
250000	2.6	14.39
330000	3.35	15.21
410000	4.1	15.74
80000	4.67	16.62
575000	5.42	17.68
700000	6.34	18.96

APPENDIX C

Synthetic Hydrograph Methodology
for Ungaged Streams

The methods described in this Appendix were developed by Dr. Kaye Brubaker, Ms. Pathak Pallavi, and Mr. Louis Guy in the Department of Civil & Environmental Engineering at the University of Maryland. This summary was provided by Dr. Kaye Brubaker (Department of Civil & Environmental Engineering, 1173 Glenn L. Martin Hall, University of Maryland, College Park, MD 20742).

Development of Discharge Hydrographs for Input to SRICOS

The SRICOS method requires a time series of flow velocity, which is generally obtained from the time series of discharge using hydraulic models. Only one of the study sites was collocated with a stream gage (White Marsh), and the 40-year flow record at that site was not long enough to give an ultimate scour depth. It was thus necessary to develop a procedure to generate long, realistic sequences of daily average flow, both for the gaged site and the ungaged sites, as input to the SRICOS program.

The original SRICOS method used USGS average daily discharge from gage data downloaded from the USGS website. A search of USGS gages found that there were gages on the stream of 4 of the 5 sites selected but that 3 of these gages were too far away from the site to be of meaningful use. Most Maryland streams do not have gages at bridge sites. Since no gage data was available for most of the sites used, a method was developed to produce long-term synthetic hydrographs that have the correct statistical distribution of daily flows.

USGS streamflow data were obtained for a number of gaging stations throughout the different geological provinces of Maryland. Only stations with a record of at least 30 years were selected. Daily discharge records in Maryland show strong seasonality in their mean, variance, and autocorrelation. The discharge (Q) data were first converted to the natural logarithm (lnQ) of daily flow. Following procedures described by Salas (1993), for each day of the year, the average and standard deviation of the lnQ across years were computed. The lnQ data were further transformed by subtracting the corresponding interannual average value from each day and dividing by that day's interannual standard deviation. The result was a sequence of zero-mean, unit variance autocorrelated deviations (Z).

The correlation of each day's Z value to the preceding day (across years) was computed. This is a measure of persistence in flow. A cosine-wave model was fit to the average lnQ, the standard deviation of lnQ, and the one-day correlation of Z. Each cosine-wave model has three parameters: mean, amplitude, and day of maximum. These nine parameters were estimated for each of the gaged watersheds.

To transfer the properties reflected by the parameters of the cosine-wave models, multiple regression was used to determine a mathematical relationship between the parameters of the cosine wave models and physical characteristics of watershed that can be determined using automated tools in GIS-Hydro 2000 (Moglen 2000). Different families of regression equations were developed for the Piedmont and Coastal Plain regions.

Synthetic streamflow hydrographs of any length for any watershed can then be generated as follows: A sequence of zero-mean, unit variance, temporally correlated deviations are generated using random sampling. A Pearson-3 (shifted gamma) distribution was found to be an appropriate distribution for standardized daily discharge (after removing the seasonal mean and standard deviation). Synthetic Z values are generated using the statistical function "Gamma Inverse" in Excel. Each synthetic Z value is multiplied by the corresponding day's standard deviation of lnQ, added to that day's mean of lnQ, to give a time series of synthetic lnQ. The lnQ values are exponentiated to obtain the time series of Q. There is no limit to the length of the synthetic hydrograph that can be produced in this manner.

The steps of data analysis and hydrograph synthesis are described below, using White marsh Run at White Marsh, Md., as an example.

The discharge (Q) data were converted to the natural logarithm of daily flow (lnQ). An intra-annual cycle in both mean and variance is observed: discharge tends to be both lower on average and more variable in the summer months. For each day of the year, the average and standard deviation of the lnQ across years were computed, as follows:

$$E[\ln Q(d)] = \frac{\sum_{\text{all } y} \ln Q(d, y)}{\text{number of years}}$$

$$\text{StdDev}[\ln Q(d)] = \sqrt{E\{\ln Q(d, y) - E[\ln Q(d)]\}^2}$$

where

y = year

d = day, 1 to 366

$Q(y,d)$ = discharge [cfs]

$\ln Q(y,d)$ = natural logarithm of Q

$E[\ln Q(d)]$ = Daily expected value (mean) of $\ln Q$

StdDev[ln*Q(d)]*=Daily standard deviation of $\ln Q$

The lnQ data were further transformed by subtracting the corresponding interannual average value from each day and dividing by that day's interannual standard deviation. The result is a sequence of zero-mean, unit variance deviations (Z).

$$Z(y,d) = \frac{\ln Q(y,d) - E[\ln Q(d)]}{\text{StdDev}[\ln Q(d)]}$$

The correlation of each day's Z value to the preceding day (across years) was computed. This is a measure of the day-to-day persistence in flow.

$$r_Z(d) = \sqrt{E[Z(d)Z(d-1)]} = \frac{\sum_{\text{all years}} Z(d,y)Z(d-1,y)}{\text{number of years}}$$

This value is computed across years on a daily basis, allowing for an annual cycle in 1-day lag correlation.

A cosine-wave model was fit to the average lnQ, the standard deviation of lnQ, and the one-day correlation of Z. Each cosine-wave model has three parameters: mean, amplitude, and day of maximum. In the following models, A_i and B_i (dimension: natural log of discharge) are the mean and amplitude of the cosine wave, and τ_i (dimension: day) represents the day of the year at which the peak value occurs. B_i is always non-negative, and τ_i takes a value between 1 and 366.

$$E[\ln Q(d)] = A_1 + B_1 \cos\left[\frac{2p}{366}(d - t_1)\right]$$

$$\text{StdDev}[\ln Q(d)] = A_2 + B_2 \cos\left[\frac{2p}{366}(d - t_2)\right]$$

$$r_Z(d) = A_3 + B_3 \cos\left[\frac{2p}{366}(d - t_3)\right]$$

For White Marsh Run, the mean lnQ reaches a maximum in early Spring (day 60), while the standard deviation of lnQ is highest in summer (day 248).

Analysis of the Z data from White Marsh indicates that they are well represented by a Pearson 3 (shifted Gamma) distribution. Further, the deviations corresponding to days of the year appear to be drawn from the same distribution. Selected percentiles for

the interannual sample of daily discharge on each day of the year were computed. These percentiles were used to determine the parameters of the distribution. Because the Z variable must have zero mean and unit variance, a single free parameter determines the shifted Gamma distribution: the distance of shift. This value was found by minimizing the maximum absolute difference between the sample and the computed percentiles (Kolmogorov statistic).

To synthesize a long sequence of daily-flow hydrographs, the following steps are followed:

A sequence of zero-mean, unit variance, temporally correlated deviations are generated using random sampling. Synthetic Z values are generated as follows:

$$Z(y,d) = \boldsymbol{r}_Z(d)Z(y,d-1) + \sqrt{(1 - \boldsymbol{r}_Z{}^2}\boldsymbol{x}(d)$$

where$\xi(d)$ is randomly sampled from the zero-mean, unit variance Pearson 3 distribution using Excel's "Gamma Inverse" function. Each synthetic Z value is multiplied by the corresponding day's standard deviation of lnQ, added to that day's mean of lnQ, to give a time series of synthetic lnQ.

The natural logs are exponentiated to obtain a time series of daily flow that has the same statistical properties as the original data. The method appears to capture the shape of event hydrographs: sudden rising limbs and more gradual recessions. There is no limit to the length of the synthetic hydrograph that can be produced in this manner.

7. REFERENCES

Abdel-Rahmann, N.M., "The Effect of Flowing Water on Cohesive Beds," Contribution No. 56, Versauchsanstalt fur Wasserbau und Erdbau an der Eidgenossischen Technischen Hochschule, Zurich, Switzerland, 1964, pp. 1-114.

American Society of Civil Engineers, "Sedimentation Engineering". Manual No. 54, 1977.

Annandale, George W. "Scour of Rock and Other Earth Materials at Bridge Pier Foundations". Golder Associates Inc., 44 Union Blvd, Suite 300, Lakewood, Colorado 80228.

Ansari, Kothyari, Rangaraju. "Influence of Cohesion on Scour around Bridge Piers". Journal of Hydraulic Research, March, 2002, Vol. 40, No. 1, pp. 717-719.

Briaud, J.-L., Ting, F., Chen, H.C., Gudavalli, R., Kwak, B.P., Han, S.W., Perugu, S., Wei, G., Nurtjahyo, P., Cao, Y., Li, Y., "SRICOS: Prediction of Scour Rate at Bridge Piers". Report 2937-1, Texas Department of Transportation , December, 1999.

Briaud, J.-L., Chen, H.C., Kwak, K.W., Han, S.W., Ting, F.C.K., "Multiflood and Multilayer Method for Scour Rate Prediction at Bridge Piers". Journal of Geotechnical and Geoenvironmental Engineering, February 2001. pp. 114-125.

Briaud, J.L., Ting, F.C.K., Chen, H.C., Han, S.W. Kwak, K.W., "Erosion Function Apparatus for Scour Rate Predictions". Journal of Geotechnical and Geoenvironmental Engineering, February 2001. pp. 105-113.

Briaud, J.-L., H.-C. Chen, Y. Li, P. Nurtjahyo, J.Wang, "Complex Pier Scour and Contraction Scour in Cohesive Soils". NCHRP Report 24-15, January 2003.

Chang, F., Maryland State Highway Adminstration, Baltimore, MD, personal conversation. (2003)

Dunn, I.S., "Tractive Resistance of Cohesive Channels,"Journal of the Soil Mechanics and Foundations Division, ASCE, No, SM3, Proc. Paper 2062, June, 1959, pp. 1-24.

Einstein, H.A., and El-Samni, E.S.A., "Hydrodynamic Forces on a Rough Wall," Review of Modern Physics, Vol. 21, 1949, pp.520-524.

Federal Highway Administration. "River Engineering for Highway Encroachments". Hydraulic Design Series Number 6, National Highway Institute, Publication No. FHWA NHI 01-004, December 2001.

Federal Highway Administration, Virginia Department of Transportation, Maryland State Highway Administration, DC Department of Public Works. "Woodrow Wilson Bridge Project, Hydrology and Hydraulic Report for Purpose of Scour Evaluation". May, 2000.

Flaxman, E.M. "Channel Stability in Undisturbed Cohesive Soils". Journal of the Hydraulics Division, March 1963, pp 87-96.

Grissinger, E.H. and L.E. Asmussen. Discussion of "Channel Stability in Undisturbed Cohesive Soils". Journal of Hydraulics Division, March 1963, pp.259-261.

Grissinger, Earl H., "Resistance of Selected Clay Systems to Erosion by Water". Water Resources Research, 1966, Vol. 2, No. 1 pp. 131-138.

Guven, Oktay, Melville, Joel G., and Curry, John E. "Analysis of Clear Water Scour at Bridge Contractions in Cohesive Soils". Transportation Research Record, 1797, Paper No. 02-2127.

Hanson, G.J., and A. Simon. "Discussion of 'Erosion Function Apparatus for Scour Rate Predictions' ". Journal of Geotechnical and Geoenvironmental Engineering, July 2002, pp. 627-628.

HEC-18, National Highway Institute Evaluating Scour at Bridges, 4th edition, Publication No. FHWA NHI 01-001, May 2001.

Henderson, F.M. "Open Channel Flow", Prentice-Hall, Inc., Upper Saddle River, New Jersey, 1966, p.411.

Kamphuis, J.W., "Influence of Sand or Gravel on the Erosion of Cohesive Sediment". Journal of Hydraulic Research, 1990, Vol. 28, No. 1, pp. 43-53.

Kuti, Emmanuel O. "Scouring of Cohesive Soils". Journal of Hydraulic Research, Volume 14, No. 3, 1976.

Leopold, Luna. "A View of the River". Harvard University Press, Cambridge, Massachusetts, 1994, p. 193.

Maryland SHA Bridge Scour Program (ABSCOUR) Users Manual, Office of Bridge Development, July 2003.

Melville, Bruce W., Chiew, Yee-Meng. "Time Scale for Local Scour at Bridge Piers". Journal of Hydraulic Engineering, January 1999, pp. 59-65.

Moglen, Glenn E., Casey, Michael J. "GIS HYDRO 2000", University of Maryland for MSHA. January, 2000.

Molinas, Abdeleayem, Abdou, Hosni, Noshi, Reiad. "Summary of Effects of Gradation and Cohesion on Bridge Scour Vol. 4, Experimental Study of Scour Around Circular Piers in Cohesive Soils". January 1996.

Parsons Transportation Group, "Scour Evaluation Study, Replacement of the Woodrow Wilson Memorial Bridge". November, 2000.

Salas, J.D. "Analysis and Modeling of Hydrologic Time Series". Handbook of Hydrology, D. Maidment, ed., chapter 19, 1993.

Smerdon, E.T., and Beasley, R.P., "Critical Tractive Forces in Cohesive Soils," Agricultural Engineering, St. Joseph, Mich., January, 1961, pp.26-29.